THE INFLUENCE OF LOW TEMPERATURE

ON THE

TENSILE IMPACT PROPERTIES OF TWO SHIPBUILDING STEELS

Thesis by

David Arthur Elmer

In Partial Fulfillment of the Requirements

For the Degree of

Mechanical Engineer

California Institute of Technology

Pasadena, California

1948

ACKNOWLEDGEMENTS

The writer wishes to express his appreciation to Professor Donald S. Clark for his helpful suggestions and criticisms in his capacity as thesis adviser and director of the impact laboratory.

The writer is especially grateful to Mr. David S. Wood and the other members of the impact laboratory staff for help in keeping the electronic and mechanical equipment working.

The impact machine and recording equipment employed in this investigation are the property of the Mechanical Engineering Department, California Institute of Technology.

Funds for the manufacture of testing fixtures and specimens and for the operation of the laboratory were provided by the David Taylor Model Basin, Washington, D.C., through Navy Contract NObs-34183, Task Order 2.

Appreciation is also extended to Mr. William Seiden for his assistance in making tests, computing data, and preparing drawings, and to my wife for typing the manuscript.

ABSTRACT

This thesis presents the results of an investigation of the influence of temperature on the tensile impact properties of two different samples of medium steel ship plate. These samples were designated as B-10 and C-10 with 0.16 percent carbon and 0.24 percent carbon respectively. Properties of these plates have been determined by static tension tests and tension impact tests at impact velocities from 10 ft/sec to 200 ft/sec, in the range of temperatures from about 80°F to -90°F. The results of this investigation indicate that ultimate strength is increased by low temperature at any impact velocity in this range, but that elongation and strain energy absorption are decreased at low temperatures, the greatest decrease occurring between 35°F and -40°F. The engineering critical impact velocity remains about the same or shows a slight increase with decreasing temperature, depending on the material. The impact velocity for zero strain propagation decreases with decreasing temperature. Some of the specimens taken from plate C-10 failed in a brittle manner in tests at -70°F at impact velocities above 100 ft/sec, while others did not. Specimens taken from plate B-10 exhibited a ductile type fracture at all temperatures and velocities. Under conditions of tensile impact, ship plate C-10 showed greater ultimate strength, elongation, and specific strain energy than plate B-10. These test results will make possible a better estimation of the behavior of structures of this material under conditions of longitudinal impact at low temperatures.

TABLE OF CONTENTS

LIST OF TABLES

LIST OF FIGURES

INTRODUCTION

The problem of the selection of materials to withstand impact conditions in machine parts and structures has been given intensive investigation for many years. The influence of low temperatures on metals has also been studied and recently is of increased interest, because engineering devices are entering regions of low atmospheric temperature.

A large amount of data has been accumulated concerning the performance of metals under static conditions of loading, including the range of temperatures down to liquid air [1]#. It has long been recognized that the properties of metals may be affected by conditions of dynamic loading, and tests have been devised to evaluate the properties of metals under dynamic or impact conditions.

About 1890, impact tests on notched bars were devised as a means of indicating the relative brittleness of engineering materials, and since that time two types of impact tests have become standardized. The Izod test utilizes a "V" notched square bar as the specimen, supported as a cantilever. The Charpy test uses a similar specimen with a keyhole notch and is loaded as a simple beam.

Numbers in parenthesis refer to references listed at the end of the text.

The influence of temperature on the energy to fracture one of these standard notched bars has been determined for a great many materials [2, 3]. The curve of variation of energy vs. temperature obtained from notched bar impact tests for a large number of materials and particularly for ferrous alloys, has the characteristic shape shown in Fig. 1.

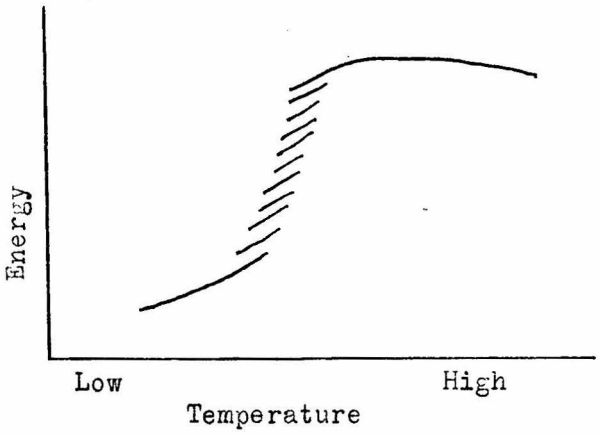

Fig. 1 The approximate relation of notched bar impact energy and temperature.

Specimens tested below the transition temperature show a greatly decreased energy to rupture.

Safety codes for the construction of pressure vessels and piping to be used at low temperature have specifications for materials based on this behavior. The temperature at which the rapid decrease in impact energy values occurs, is influenced by steelmill practice and heat treatment. In the case of mild steel, the method of deoxidation; the carbon, sulfur, phosphorus and gas content; the number, size, and distribution of non-metallic

particles; the grain size; the heat treatment; and the degree of cold work, all influence the transition temperature.

It is recognized that the notched bar test determines the properties of a material for the constraint imposed by the shape of the bar and notch and may have very little value for properties under a different constraint. This makes notched bar impact data difficult or impossible to use directly in design. Two examples of this inconsistency are presented here. Two samples of steel which had slightly different analyses and heat treatments and approximately the same values of ultimate tensile strength and standard Charpy impact values showed widely different results when the width of the impact test bar was doubled. Here both materials flowed and gave ductile fractures under the constraint of the standard width Charpy specimen, while under the constraint of the double width notched bar, only one was ductile. The other failed in a brittle manner with very small absorbtion of energy. In the case of railroad rails and frogs, some materials have been used under severe impact conditions for long periods of time at temperatures well below the notched bar impact transition temperature, with no failures, while others have failed.

The reason for this behavior can be explained by the mechanism of deformation of metals. Metals under stress may deform plastically by slip or twinning or fracture by cleavage.

The stress which produces these different deformations is different at different temperatures. In ductile materials the stress for slip is low and deformation by slip takes place, causing cold work and a change in orientation of the grains, until these effects cause the stress required to produce slip to be higher than that for cleavage. In more brittle materials the difference between the slip and cleavage stresses is smaller, so cleavage occurs sooner, and in some cases the stress for slip is higher than for cleavage and practically no plastic deformation takes place before rupture. Deformation may also take place by twinning, but the amount is small compared to slip, and the stress at which this occurs is about the same as for cleavage [4].

In the case of a notched bar in bending, the material is constrained by the shape of the notch so that deformation by slip can occur only near the surface of the material and the stress is quickly raised to the point of cleavage. As the temperature is decreased the stress for deformation by slip may increase while that for cleavage may remain about the same. The result is that at some certain temperature there is no deformation by slip and a brittle failure takes place with very low absorption of energy.

Realizing the limitations imposed on the use of notched bar impact data by the stress constraint, different investigators [5-11] have devised tension and compression impact tests in an attempt to determine impact properties of materials, rather than the notch sensitivity or the influence of a certain stress configuration.

In these tests, short cylindrical specimens were tested under conditions of longitudinal impact and ultimate strength, elongation, and energy to rupture were measured. In most of the tests, ultimate strength, elongation, and energy were found to increase with increasing impact velocity and, in some cases, above a certain critical velocity, the energy decreased with increasing impact velocity. Some of the authors [9,10,11] attempted to determine impact properties as a function of the average strain rate. The specimens used in these early tests showed little change of elongation and energy with change in impact velocity.

There was considerable disagreement between data obtained by different investigators, and no clear understanding of the principles involved in longitudinal impact until 1941.

In 1941, as a result of the desire for basic information on the dynamic performance of metals in general, and a solution to the problem of the absorption of the energy of shock waves in connection with bomb proof shelters in particular, Th. von Kármán [12,13] conceived a theory for the propagation of plastic strain waves in solids. Experimental verification of the theory was obtained from tension, compression, and bending impact tests made in 1942, 1943, and 1944 [14,15]. These tests led to a clear concept of a critical impact velocity [16], and to analytical and

graphical methods of solution of problems in longitudinal and transverse impact [17].

More recently the David Taylor Model Basin, U.S. Navy Department has sponsored an investigation at the California Institute of Technology on the influence of low temperature on the tensile impact properties and on the critical impact velocity of steel. Preliminary tests were made on an annealed 0.19 percent carbon steel [18]. As the result of these tests, modifications were made in the specimen shape and testing fixtures; to permit the critical velocity to be as clearly defined as possible, and to give a more uniform temperature along the length of the specimen.

The purpose of this thesis is to present the results of an investigation on the influence of temperature on the tensile impact properties of two ship plate steels, and the results of a comparison between the dynamic properties of two steel plates with similar static properties.

FUNDAMENTAL CONSIDERATIONS

The concept of the propagation of elastic strains in a long prismatical body subject to longitudinal impact is old. This problem was analysed by Thomas Young [19], who established the proportionality between velocity of impact and elastic strain. This relation is given by the following formula:

$$v_i = C_0 \varepsilon \quad ,$$

in which v_i is the impact velocity and ε the resulting elastic strain. C_0 is the velocity of propagation of the deformation.

$$C_0 = \sqrt{E/\rho} \quad ,$$

where E is the modulus of elasticity and ρ is the mass density of the material. Young observed that when the impact velocity v_i is high enough, plastic strain is induced near the point of impact. No systematic attempt was made to determine the relations of stress and strain above the elastic limit caused by longitudinal impact, either by Young or subsequent investigators.

Th. von Kármán [12,13] extended the understanding of the propagation of waves in bars by his development of the differential equation of equilibrium. He considered the coordinates from the Lagrangean point of view, and related stress to strain by a modulus of deformation $\frac{d\sigma}{d\varepsilon}$, which is not a constant, but is a function of the strain. The solution to

this equilibrium equation leads to relations similar to Young's.

$$v_1 = \int_0^{\varepsilon_1} C\,d\varepsilon$$

$$C = \sqrt{\frac{d\sigma}{d\varepsilon}/\rho}$$

The above equations are only true for the case of very long bars, but by considering the stress-strain relations during unloading as elastic, the theory and methods of solution can by extended to bars of finite length and with varying cross sections. However, this extension is not necessary for an understanding of the principles. The above relations can be used for the solution to problems of longitudinal impact. The slope of the engineering stress-strain diagram provides the values of $\frac{d\sigma}{d\varepsilon}$ as a function of strain; so a graphical solution can be obtained [17].

It is apparent that at the point of ultimate strength the slope of the engineering stress-strain diagram will be zero and the velocity of propagation for strains of this magnitude will be zero. This leads to the concept of a critical impact velocity, which is defined as the velocity corresponding to the strain which propagates at zero velocity. The critical velocity of practical engineering application is the impact velocity above which the energy and elongation to rupture decrease rapidly and failure occurs near the point of impact. This will hereafter be referred to as the engineering critical impact velocity.

In some materials this point is sharply defined, while in others there is only a gradual decrease in energy and elongation as impact velocity is raised above the critical value.

The solution of longitudinal impact problems, using the engineering stress-strain diagram for the relation of $\frac{d\sigma}{d\varepsilon}$ as a function of strain, is based on the assumption that the static stress-strain curve represents the relations of stress to strain under impact conditions. This is doubtful, as it has been deduced from impact tests on long iron wires [15], uniaxial strain tests on ship plate steel [20], rapid loading tests on SAE 1015 hot-rolled steel [21], and other considerations that the shape of the stress-strain curve changes under conditions of impact loading. This is particularly evident in the case of ferrous alloys which show a yield point. In addition to this, the above relations as a solution of problems of longitudinal impact are good only for continuous, single valued functions of $\frac{d\sigma}{d\varepsilon}$. The discontinuous yield point exhibited by low carbon steel clearly violates this requirement. For these reasons the graphical solution is limited in accuracy and was not used in this investigation.

The force-time relation obtained at the fixed end of the specimen during a tensile impact test can be understood by the consideration of plastic strain propagation. The force-time relation cannot be transformed into one of stress-strain, because the rate of strain in the specimen is not proportional to velocity, but varies from zero to a very high value as the strain wave proceeds along the specimen. The shape of the force-time diagram

is easily explained. From the moment of impact and for the interval of time t_o, force is zero at the fixed end. The time t_o is the time for the elastic wave to travel the length of the specimen. At time t_o the force at the fixed end increases suddenly to a certain value. This force is greater than the elastic limit, because a strain wave reflection from the fixed end adds to the incident wave. The force increases progressively from further reflections and from the slower plastic strain wave until a maximum is reached. This maximum value is held until a very short time interval after rupture when the force drops to zero. The time interval after rupture is the time for the elastic unloading wave to travel from the point of rupture to the fixed end.

With the understanding of the fundamentals of the mechanism of elastic and plastic strain propagation, a proper analysis of the experimental data obtained in this investigation can be made.

EXPERIMENTAL INVESTIGATION

A. Material Tested

The material used in this investigation came from two samples of 3/4 in., hot-rolled, medium steel ship plate. These samples were obtained from the University of California at Berkeley. One sample, manufactured by the Bethlehem Steel Co., was designated B-10; the second sample, manufactured by the Carnegie-Illinois Steel Co., was designated C-10. The following report of analysis, properties, and treatment was obtained from the Mechanical Engineering Department, University of California, by letter of June 12, 1947:

Analysis	B-10	C-10
Carbon %	0.16	0.24
Manganese %	0.74	0.49
Silicon %	0.03	0.043
Phosphorus %	0.011	0.015
Sulphur %	0.030	0.033
Nitrogen %	0.005	0.009

Properties		
Yield Point lb/in.^{2}	35,800	39,000
Ult. Strength lb/in.^{2}	59,600	67,400
Elongation in 8 in. %	26	25.5

Deoxidation Practice B-10		Deoxidation Practice C-10	
Ferro Manganese lb/ton	8½	80% Ferro Manganese lb/ton	6
Ferro Silicon lb/ton	1-1/8	50% Ferro Silicon in ladle lb/ton	2.6
Aluminum Silicate in ladle lb/ton	2½	Aluminum added to mold lb/ton	1/3
Small amount Aluminum added to mold			

The structures of the plates are shown in the photomicrographs, Figs. 2 and 3. The structure of these plates consists of ferrite and pearlite with a number of small inclusions, C-10 having about twice as much pearlite, because of its higher carbon content. The structure of B-10 shows elongated ferrite grains, with the pearlite arranged more or less in layers as the result of rolling. C-10 shows no such arrangement. The ferrite grain size is approximately ASTM No. 6 for both materials. The average hardness was Rockwell B 55 for plate B-10 and Rockwell B 74 for plate C-10.

These hardness values were obtained as the result of hardness tests made on 20 specimens from plate B-10 and 11 specimens from plate C-10 selected at random. The specimens were cut off at the dynamometer-end shoulder. Four hardness measurements were made on each specimen in such a manner as to preclude more than two points being in the central plane of the plate. The average of these four readings was taken as the specimen hardness and the average of all specimens as the plate hardness. Specimen hardness did not vary from plate hardness by more than 4 points Rockwell B for plate B-10 and 3 points Rockwell B for plate C-10.

The plates were oxy-acetylene torch cut into sections, and then bars 3/4 in. wide by 10½ in. long were sawed out

Fig. 2 Photomicrograph of ship plate steel B-10. Nital etch, X100.

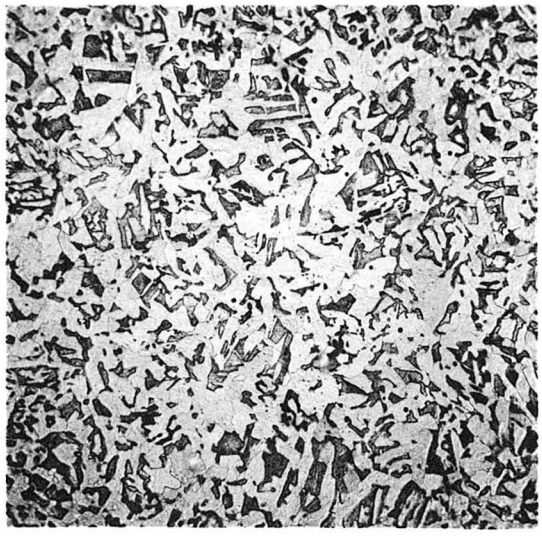

Fig. 3 Photomicrograph of ship plate steel C-10. Nital etch, X100.

of the sections. All portions of the plates within one inch of the torch cut edges were sawed off and discarded. Test specimens were machined from the bars, with the axis of the specimen parallel to the direction of rolling, to the dimensions shown in Fig. 4. The gage portion of the specimens was finished by grinding to a surface roughness between 10 and 25 μ in. RMS, with variation on individual specimens within 4 μ in., as determined with a Brush Development Co., Model SA-2, Surface Analyser.

Specimen dimensions were selected to satisfy the limitations of the equipment and to provide a proper ratio of length to diameter that will clearly define the critical velocity [22,23]. The slots in the tup-end threads are to admit the cooling fluid.

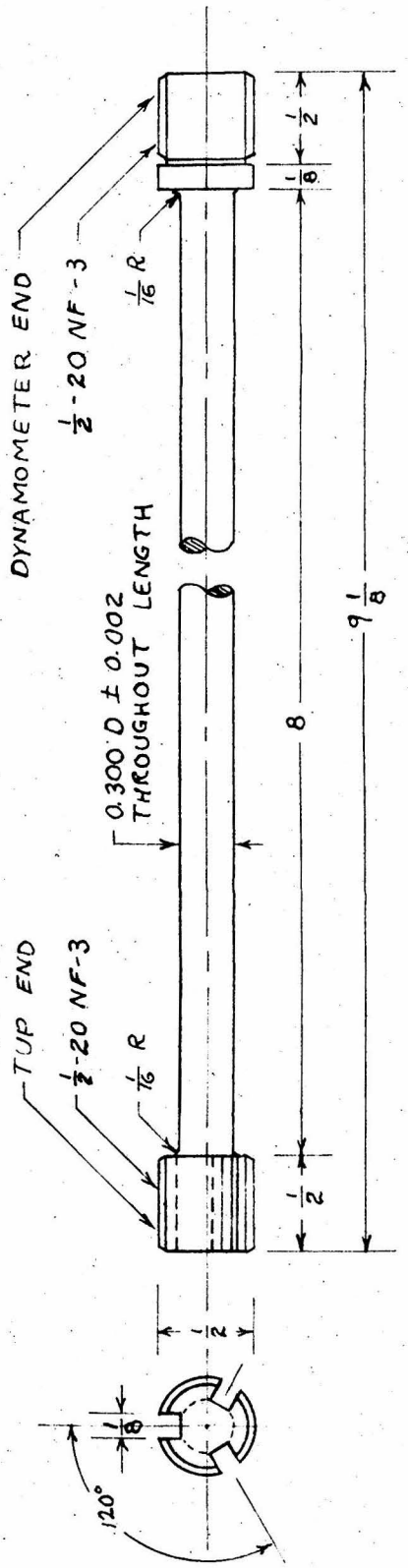

Fig. 4 Test specimen for tension and tension impact tests.

B. Equipment and Procedure

(a) Outline of Tests

Static tension and tension impact tests were made at four different temperatures: 70°F, 35°F, -40°F, and -70°F. A few additional impact tests were made on the B-10 material at temperatures of about 0°F.

Load and elongation were measured at a constant temperature during the static tests. Tension impact tests were made at impact velocities of 10, 25, 50, 75, 100, 125, 150, 175, and 200 ft/sec, at each of the temperatures. A record of the force vs. time at the fixed end of the specimen was obtained and the final length of the specimen was measured.

(b) Static Tests

Static stress-strain data were obtained from tests made with a 30,000 lb Riehle universal testing machine. A photograph of the static test assembly is shown in Fig. 5. The stress was computed from the load on the specimen and the original cross sectional area. Strain measurements were obtained with two dial gages mounted on opposite sides of the specimen. The specimen, with testing fixtures, is shown in Fig. 6. These gages measure the total elongation in the 8 in. gage length, plus the deformation in the shoulders and threads

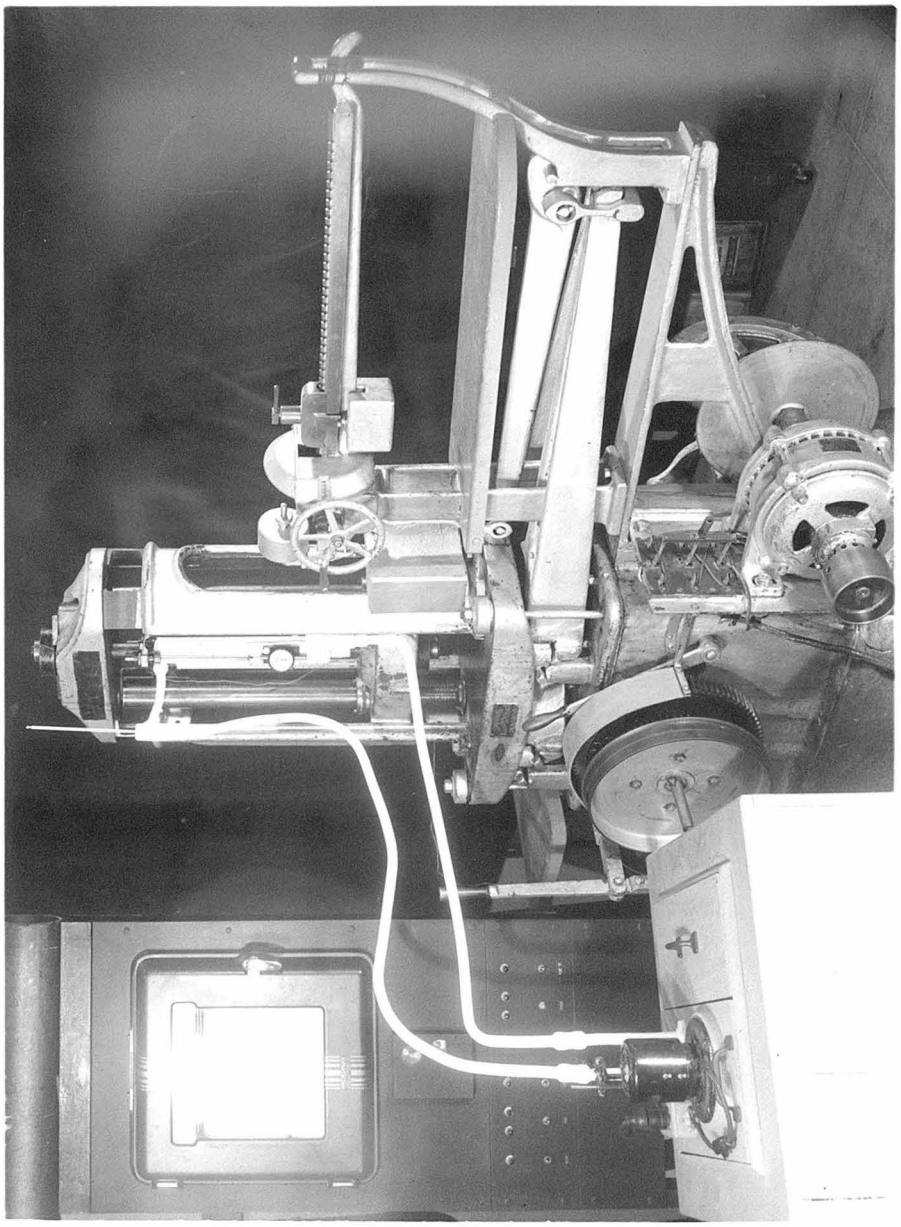

Fig. 5 Photograph of testing machine with static test assembly.

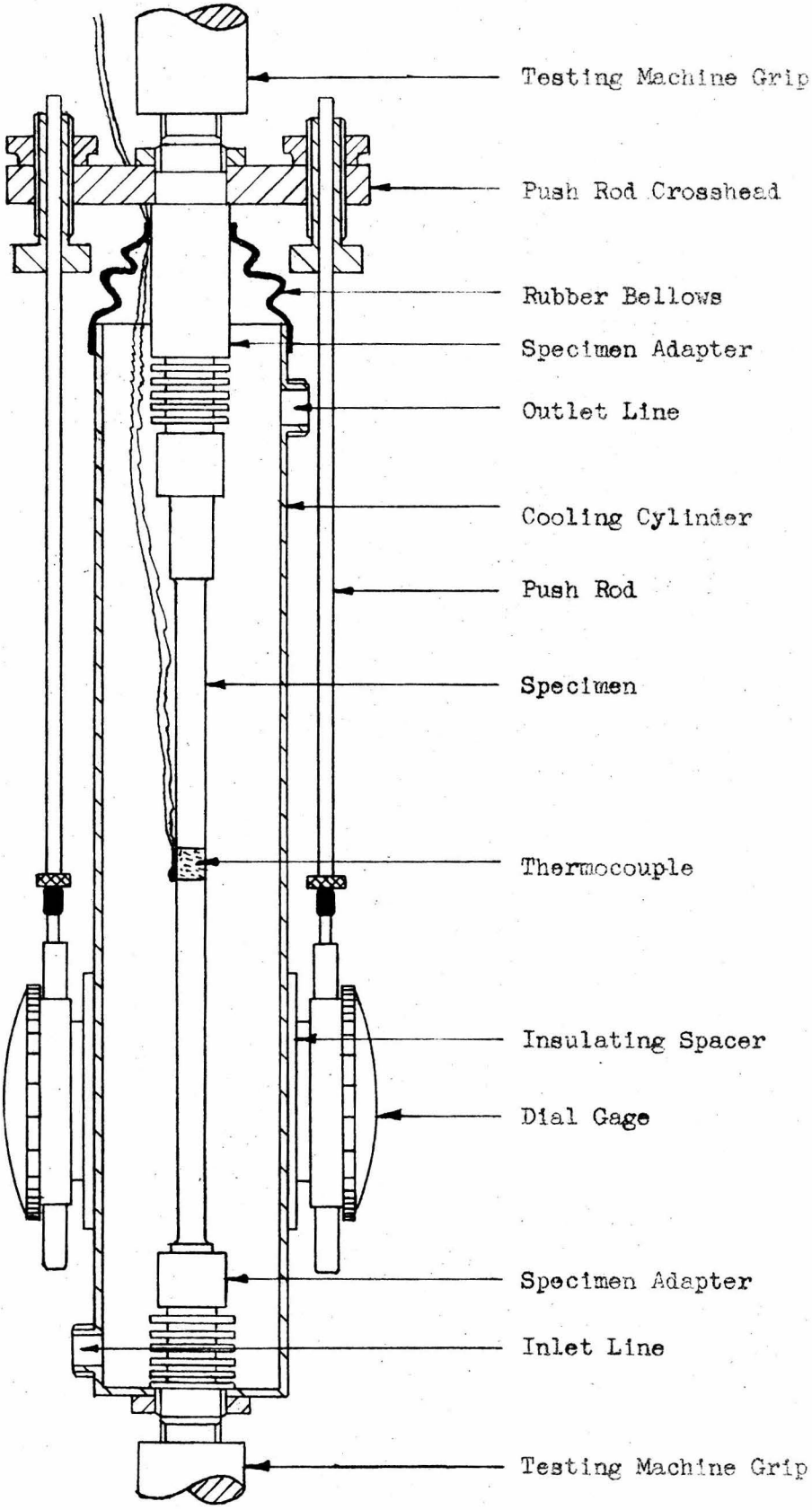

Approximately Half Size

Fig. 6 Assembly of specimen and static testing fixtures.

of the specimens and in the fixtures. For a more accurate determination of strain, a Huggenberger extensometer with a 20 mm gage length was used in the first part of the tests at room temperature. These tests were made very slowly, taking about two hours for each test. The specimens were allowed to creep for about two minutes after the load was applied before reading load and elongation so that equilibrium conditions would be approximated.

The static yield point and ultimate strength were determined with an accuracy within ± 2 percent and ± 1 percent respectively. The dial gage readings for elongation were in error by the amount of elongation in the specimen shoulders and threads and in the fixtures. This can be corrected by assuming that the strain outside of the gage length is elastic and proportional to the load. Using $E = 29 \times 10^6$ lb/in.^{2} for the specimen, obtained with the Huggenberger extensometer as the basis for the correction, the total static elongation can be determined within ± 1 percent. This correction was not made because it amounts to only about 3 percent, which is well within the normal scatter encountered in total elongation. Reduction of area was determined to within about ± 3 percent by measuring the diameter of the necked-down section of the specimen with point micrometers after rupture. Specific energy was determined from the area within the stress-strain

curve to within ± 4 percent.

The cooling system consists of an insulated box containing a stainless steel tank. A small reservoir is provided within this tank and connected to a centrifugal pump and copper heat exchange coil. The tank is filled with a mixture of dry ice and denatured ethyl alcohol. The reservoir is filled with denatured ethyl alcohol. The pump circulates the alcohol through the coils placed in the tank containing the cold mixture, through tubing to a brass cylinder surrounding the specimen in the Reihle testing machine, and back to the reservoir. The above system was used for tests made at approximately -90°F. For tests at approximately -45°F, the number of coils in the cold mixture was decreased and a number of coils were inserted in the coolant line ahead of the specimen cooling cylinder. These coils were heated by placing two 150 watt incandescent lamps at their center. For tests at 32°F, the specimen was cooled by circulating water directly from the tank containing a mixture of ice and water, then through the cylinder around the specimen and back to the tank. No cooling or heating was required for the 70°F tests. Specimen temperatures were determined by means of a copper-constantan thermocouple and a Leeds and Northrup micromax recording potentiometer. The thermocouple and potentiometer combination was calibrated using equilibrium mixtures of ice and water, and dry-ice and ethyl alcohol as temperature standards. The thermocouple was held in contact

with the center of the specimen with rubber tape. The temperature of the coolant was measured by thermometers in wells at the inlet and outlet of the cylinder surrounding the specimen to indicate when thermal equilibrium prevailed.

Temperature variation during the static tests was less than $\pm 3^{\circ}F$, except for the $-45^{\circ}F$ tests where the variation was within $\pm 5^{\circ}F$. The Micromax scale indicated temperatures to an accuracy within $\pm 1.5^{\circ}F$. During the tests the temperature differences between the center and the ends of the specimens were found to be of the order of $0.2^{\circ}F$.

(c) Impact Tests

The impact machine used in this investigation consists of a 350 hp hydraulic impulse turbine wheel 44 in. in diameter on the shaft of a direct current motor. The buckets have been removed from the wheel and striking jaws and counter-weights added. The total weight of the rotating parts is approximately 2000 lb. The motor, wheel, and jaws are shown in Fig. 7. The test specimen is mounted horizontally below the wheel with one end screwed into a force measuring dynamometer. The dynamometer is screwed into a 715 lb. steel block which slides in ways securely fastened to the floor. The steel block is moved on the ways to place the unsupported end of the specimen between the jaws of the wheel and into position for the impact, and then the block is firmly clamped in place.

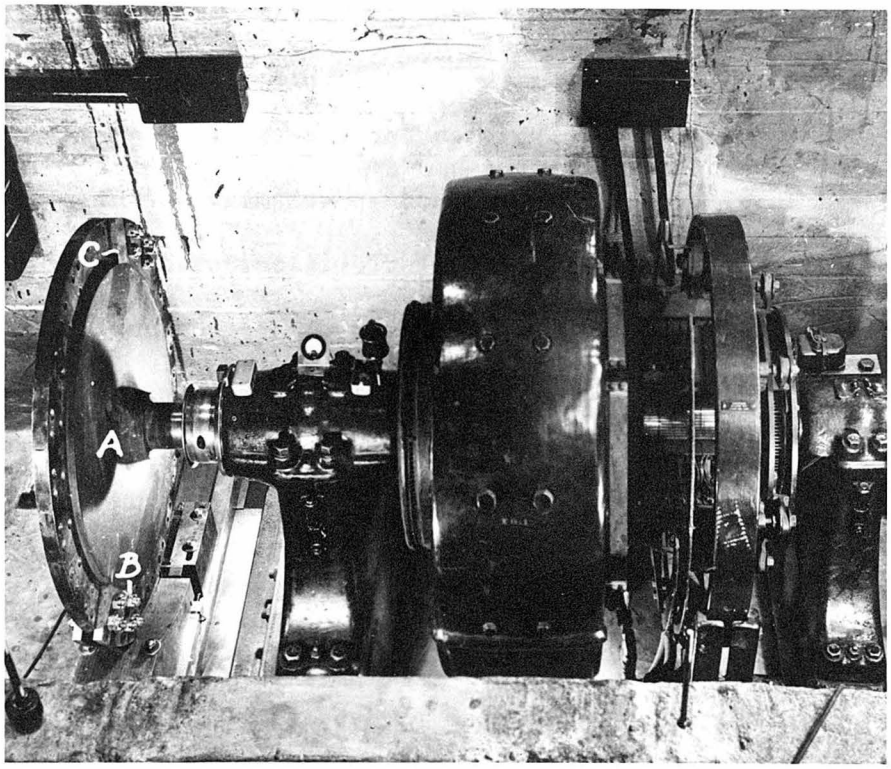

Fig. 7 Photograph of rotary impact testing machine.

The dynamometer is made of heat treated AISI 440-C stainless steel with 4 Baldwin Southwark, AB-14 strain gages in series cemented to a hollow cylindrical section. The resistance sensitive elements of the gages are parallel to the axis of the specimen. A flange on the dynamometer serves to hold a brass cooling cylinder around the specimen. Axial fins are present to assist in the transfer of heat from the heavy steel block in low temperature tests. The dynamometer was calibrated on a static tension testing machine with a sensitive Wheatstone bridge to an accuracy within ± 5 percent at $75^{\circ}F$ and at $-83^{\circ}F$. The difference in the calibration at the two temperatures is less than the 5 percent measuring error. Calibration curves for the dynamometer are shown in Fig. 8. This small effect of temperature is in agreement with data reported by Campbell.[24)]

A square tup is screwed onto the unsupported end of the specimen and locked in position. When the wheel is at the desired speed, a strong spring is released by a solenoid-operated trigger which brings a yoke up around the specimen, between the tup and the striking jaws. The jaws strike the yoke, which, in turn, strikes the tup producing the impact and the unsupported end of the specimen is pulled at the tangential velocity of the wheel to failure. A brush and commutator system on the wheel shaft permit the yoke to be moved only when the striking jaws are in the proper position. After rupture, the end of the

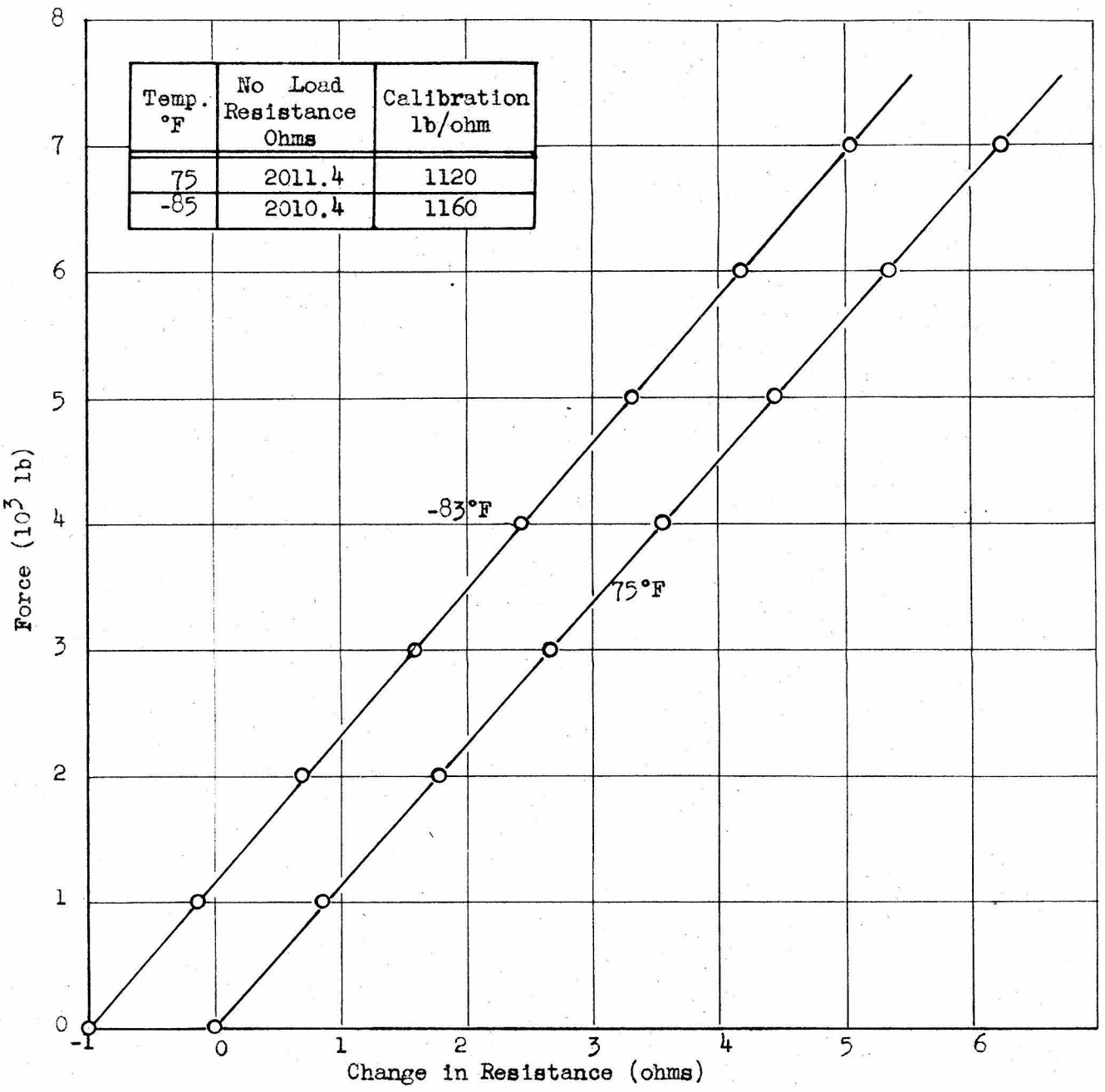

Fig. 8 Calibration curves for low temperature impact test dynamometer No. B at 70°F and -83°F.

specimen, tup, and yoke are caught in a bin of cotton waste. A diagram of the details of the specimen and accessories, mounted in the rotary impact machine, is shown in Fig. 9.

A "strobotac" is used in conjunction with appropriate markings on the side of the rotating wheel to measure the impact velocity. The tangential velocity of the jaws is determined from the speed of the wheel and the distance from the center of rotation to the point of impact. This measurement is accurate to within ± 1 percent. The kinetic energy of the wheel is such that the decrease of velocity during the test, caused by the energy required to rupture the specimen, is 25 percent at 10 ft/sec, 5 percent at 25 ft/sec, and 0.3 percent at 100 ft/sec.

For low temperature tests a cylinder is placed around the specimen and cooled denatured ethyl alcohol pumped through it as in the static tests. The fluid enters through slots in the tup-end threads, passes over the specimen, and leaves the cylinder at the dynamometer end.

Temperature is measured with a copper-constantan thermocouple held on the specimen with rubber tape, and the Leeds and Northrup Micromax used in the static tests. The arrangement of the equipment for the low temperature impact tests is shown in Fig. 10. The cooled alcohol is circulated until the system is in equilibrium as indicated by a thermometer in the outlet line and by the Micromax record. Then the rotating wheel is brought up to speed

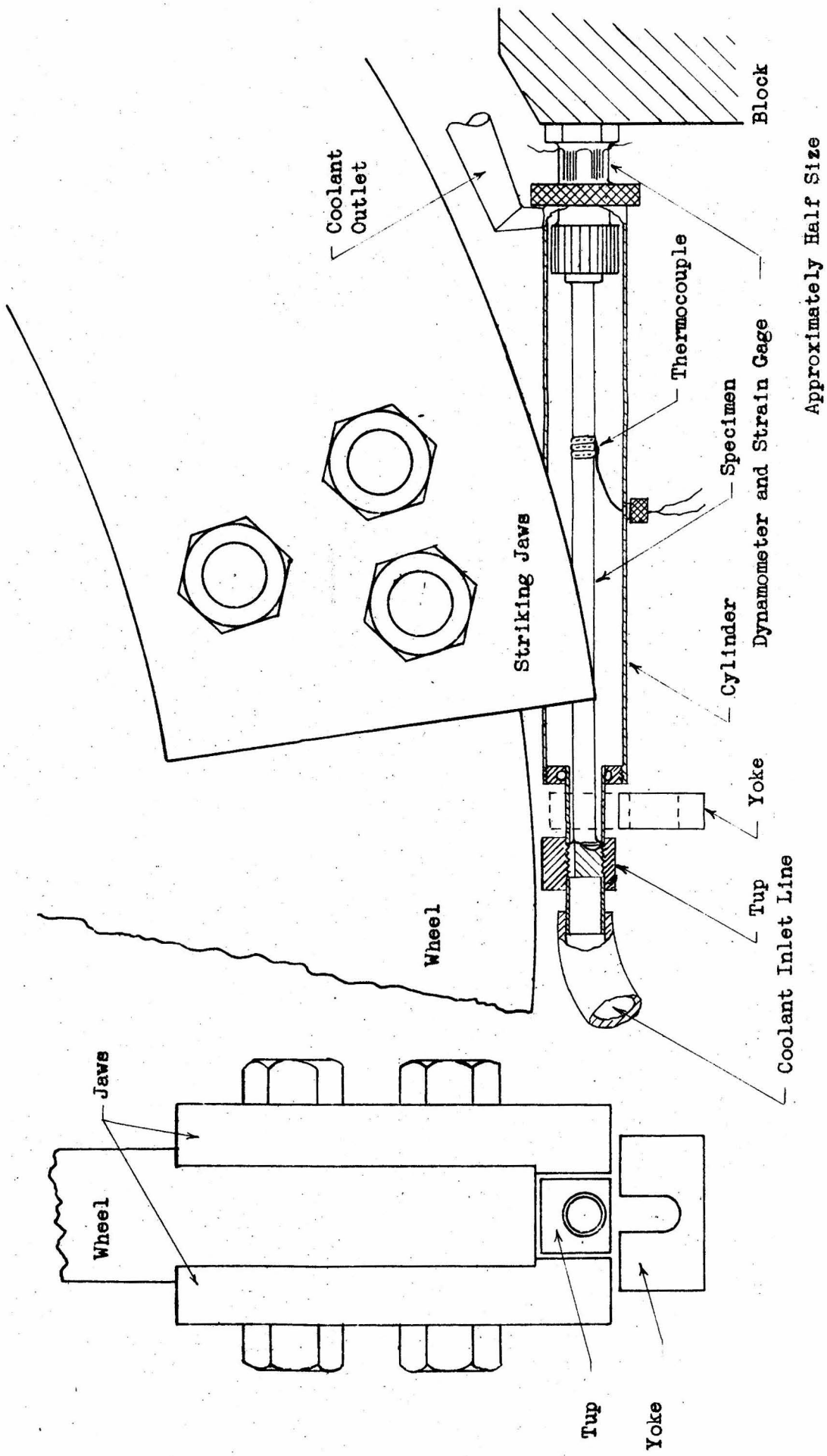

Fig. 9 Assembly of impact test specimen and fixtures.

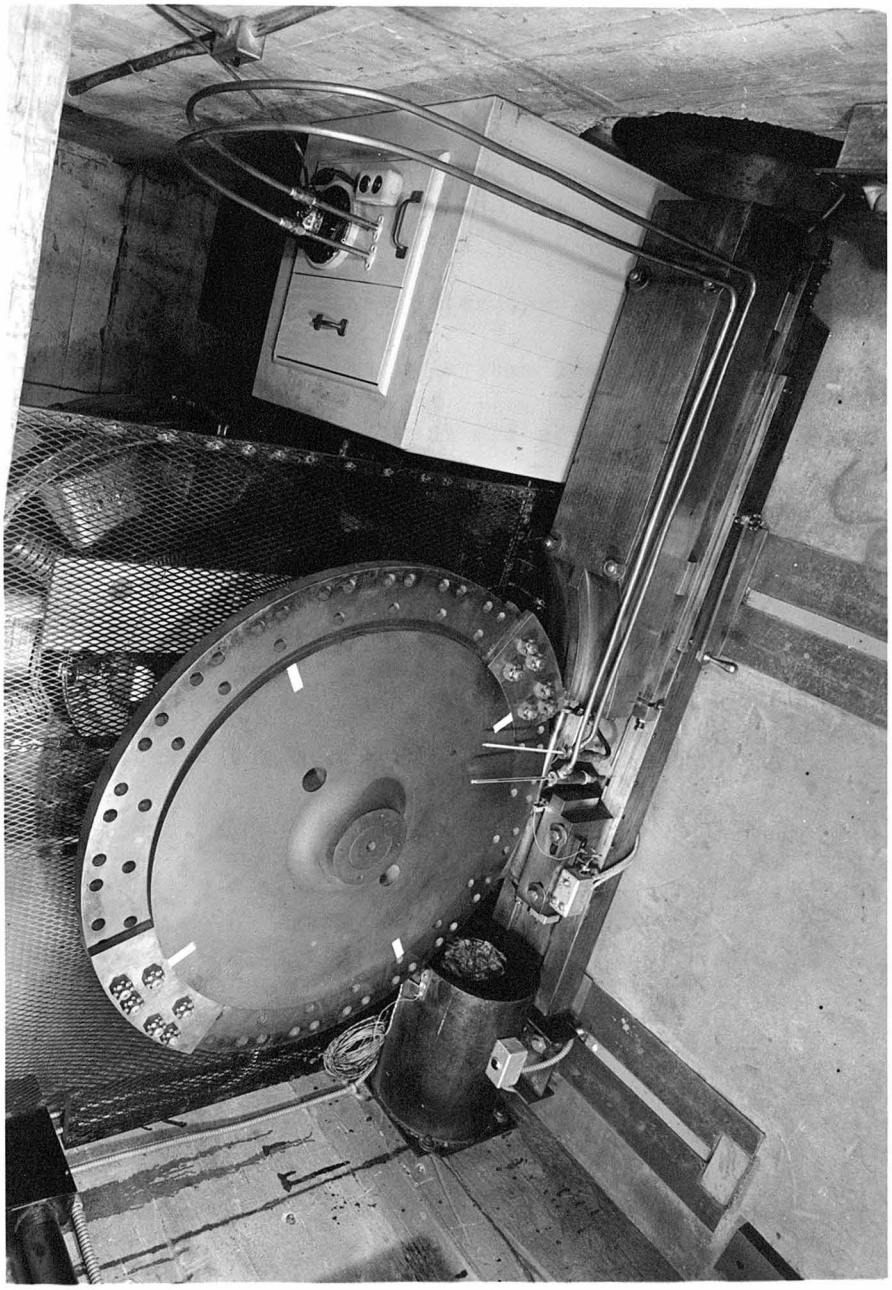

Fig. 10 Photograph of impact machine with specimen assembly and cooling equipment.

and the test made. The air circulated by the rotating wheel, while coming up to speed and in the few moments while final adjustments are being made, warms up the system enough to raise the temperature of the specimen 2 to 10°F for the low temperature tests. This also causes a temperature difference between the fixed and moving end of the specimen of about 0.5°F for tests at velocities of about 25 ft/sec and about 5°F for tests at about 150 ft/sec. Immediately after the specimen is ruptured, valves in the coolant circulating system are closed.

All recording equipment and actuating controls are centered in the recording and control unit shown in Fig. 11. The recording system consists of a strain gage bridge, amplifier, sweep generator, timing system, RCA Type 327-A Cathode Ray Oscilloscope, camera, and power supplies, and other auxiliary equipment. The control unit contains the operating controls for the rotary impact machine and other equipment not concerned with this investigation. The recording system is used to record force on the dynamometer vs. time during impact. A schematic diagram of the recording system is shown in Fig. 12.

The dynamometer strain gage is one leg of a 1:1 voltage dividing circuit. The second leg is a dummy gage of similar mechanical construction to provide a voltage divider having symmetrical characteristics with respect to temperature drift, capacity, and inductance. The strain gage signal is calibrated

Fig. 11 Photograph of control and recording unit.

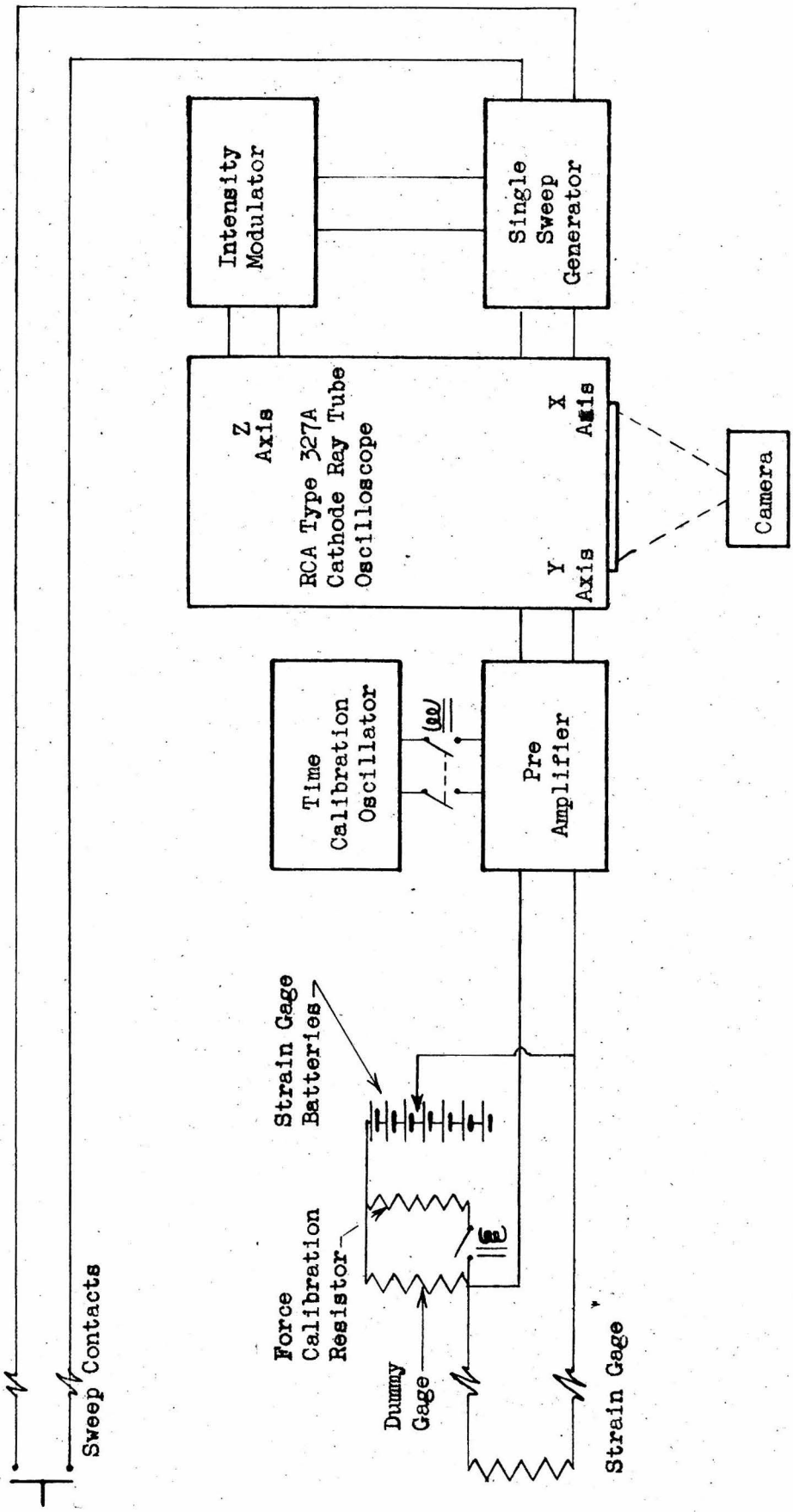

Fig. 12 Schematic block diagram of the recording system.

by shunting a known resistance across the dummy gage during a single sweep of the oscilloscope. The sweep initiation and the closing of the calibration switch are synchronized with relays to make a vertical step in the trace on the oscilloscope screen. By knowing the resistance of the calibration resistor, the strain gage and the dummy gage, the gage calibration in lb/ohm, the height of the vertical step on the calibration sweep can be computed in pounds. The force on the dynamometer during the impact can be computed by comparison of the vertical deflection of the force-time diagram with the calibration trace. A timing calibration is provided by the time calibration oscillator, which supplies a separate single sweep with sharp vertical "pips" on the oscilloscope screen just below the force calibration base line. The timing oscillator consists of a Hewlett-Packard, Model 200-C variable frequency oscillator and a differentiating circuit, to convert the sine wave output of the oscillator into sharp-peaked time "pips" at the same frequency. For accurate setting, the variable frequency oscillator signal is compared with a signal from a Hewlett-Packard, Model 100-A Crystal oscillator by means of an auxiliary oscilloscope.

The maximum sensitivity of the oscilloscope is approximately 70 mv/in. and the average signal from the strain gage is 120 to 220 mv, making a record on the oscilloscope screen approximately 2 in. high. To take full advantage of the 9 in. screen on the

oscilloscope, a capacity coupled, DC pre-amplifier with a fixed gain of about 10 is used with the oscilloscope gain and strain gage battery voltage slightly decreased.

The sweep is initiated during the test by the jaws of the impact wheel striking a contact wire on the yoke. An intensity modulator is used in conjunction with the sweep generator to blank out the beam in the cathode ray tube at all times except during a sweep. The impulse required to turn on the oscilloscope beam is supplied by the sweep generator.

The oscilloscope screen is photographed on 35 mm Eastman Linograph Ortho film, using a special stationary film camera with a Zeiss Biotar f:1.4 lens. The record consists of three traces on a single frame of film: a vertically stepped calibration trace, a horizontal timing trace, and a force-time record from the dynamometer strain gage. Enlarged tracings from typical oscilloscope records are shown in Fig. 13. A robot control is incorporated in the recording unit which operates the room lights and camera shutters, applies the timing and force calibrate traces, and triggers the impact yoke; performing these functions in the proper sequence.

To analyze the data, the 35 mm film records are projected with an enlarger to about 7.5 diameters and traced on cross-section paper. From this record and from the original dimensions of the specimen, the stress-time relationship at the fixed end

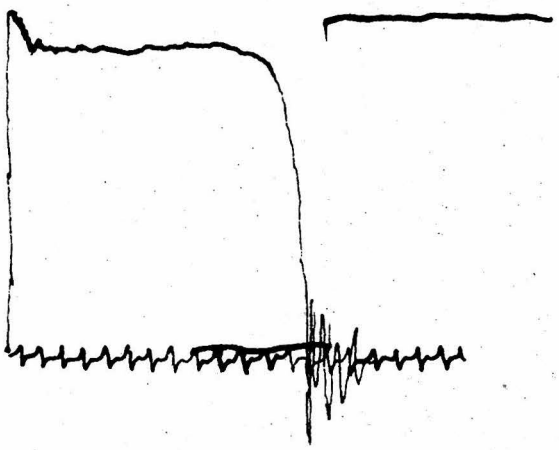

Calibration step 5150 lb
timing frequency 1000 c/sec
ultimate strength 66000 lb/in.^{2}
elongation 14.4% in 8 in.
specific energy 790 ft lb/in.^{3}

(a) Ship plate specimen 55B tested at -78°F, impact velocity 10.1 ft/sec

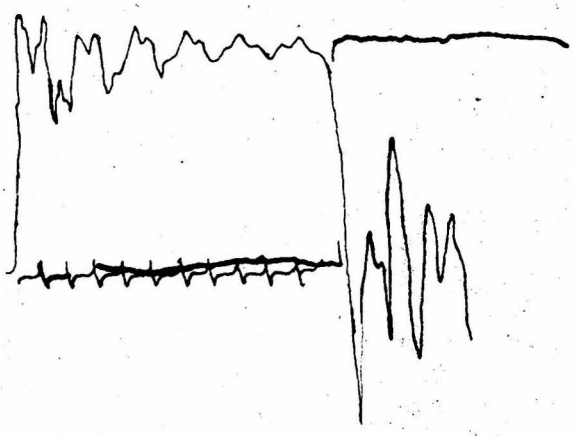

calibration step 6420 lb
timing frequency 5000 c/sec
ultimate strength 89000 lb/in.^{2}
elongation 15.8% in 8 in.
specific energy 1170 ft lb/in.^{3}

(b) Ship plate specimen 59C tested at -70°F, impact velocity 49.8 ft/sec

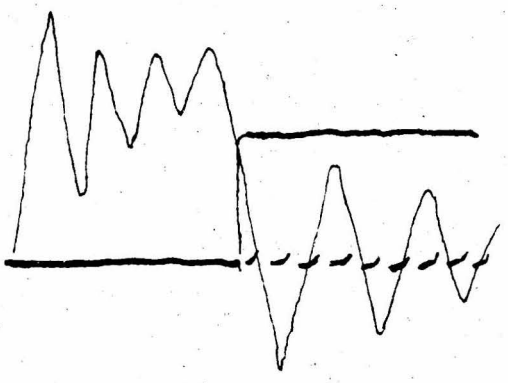

calibration step 3940 lb
timing frequency 15000 c/sec
ultimate strength 76000 lb/in.^{2}
elongation 11.5% in 8 in.
specific energy 730 ft lb/in.^{3}

(c) Ship plate specimen 48C tested at 74°F, impact velocity 199.9 ft/sec

Fig. 13 Tracings of typical oscillograph records of tensile impact tests. Enlarged about 3 times.

of the specimen is determined. This measurement of stress is subject to errors in measuring the specimens, measuring the displacement of the force-time record and the calibration step, and to errors introduced by the electronic system, and subject to the limitations of frequency response of the electronic and mechanical system. An irregular sine wave is superimposed on the force-time record which is damped out before the end of the longer tests. This transient oscillation is caused by lateral vibrations of the specimen and longitudinal vibrations of the dynamometer. The contribution from each source can be identified from the frequency of the oscillations. The cross sectional area of the specimen can be determined within about ± 1 percent. The amplitude of the irregular sine wave in the force-time record is often very large, making the measurement of the maximum average force subject to a possible error of 2 to 10 percent. The height of the force calibration step can be measured to within ± 5 percent. The frequency response of the entire system from strain gage to oscilloscope screen is flat to within 4 percent from 20 to 100,000 cycles. It is reasonable to assume that the gage sensitivity and Young's modulus for the dynamometer are not affected by the impact velocity. This leads to an overall possible error in determining the ultimate strength of from ± 10 to ± 20 percent depending on the force-time record.

The total elongation was determined from measurement of the original and reconstructed gage length of the specimen to within ± 1 percent when there was 20 percent elongation. This measurement is less accurate for less elongation. Elongation can be computed from the length of the force-time record, the timing calibration and the impact velocity, but the length of the record is sometimes uncertain since the sweep may be initiated after the instant of impact. The length of record can be measured to within about ± 5 percent and the timing calibration to about ± 2 percent, making the possible error in these elongation measurements at least ± 7 percent. For greater accuracy, elongation was therefore determined from the reconstructed length of the specimen.

Specific energy was determined by integration of the force-time diagram. A correction was made on the length of the diagram when in disagreement with elongation as determined from the reconstructed length of the specimen. This method allows a possible error of ± 5 to 13 percent depending on the diagram.

C. Test Results

(a) Static Tests

The results of the static tensile tests are given in Table I and the static stress-strain curves are presented in Figs. 14, 15, 16, and 17. Curves showing the variation of static ultimate strength, yield point, elongation, and specific energy with temperature are presented in Fig. 18. As the temperature is lowered, the yield point and ultimate strength are increased, total elongation remains essentially constant, producing about the same increase in specific energy as in ultimate strength. The shape of the stress-strain curved is not changed by reducing the temperature. Reduction of area is slightly lower at low temperatures.

Plate B-10 has an ultimate strength of about 50,000 lb/in.^{2} at 75°F, this is increased to about 55,000 lb/in.^{2} at -90°F. Plate C-10 has higher strength and lower elongation and reduction of area than B-10 as is expected from their respective carbon contents. C-10 has an ultimate strength of about 65,000 lb/in.^{2} at 77°F, this is increased to about 73,000 lb/in.^{2} at -90°F.

(b) Impact Tests

The results of tensile impact tests on the two materials are given in Tables II through X. Curves of ultimate strength, elongation, and specific energy vs. impact velocity, for each temperature, are given in Figs. 19 and 20. Because of the

TABLE I

RESULTS OF STATIC TENSION TESTS ON SHIP PLATE STEEL

Spec. No.	Temp. deg. F	Yield Point $lb/in.^2$	Ultimate Strength $lb/in.^2$	Elong. Percent in 8 in.	Specific Energy $ft\ lb/in.^3$	Reduction of Area Percent
7B	76	26400	51800	25.8	1008	68.6
8B	77	23900	48200	28.7	1078	66.4
5B	31.5	26000	51000	26.7	1020	66.4
6B	32	24800	50000	26.1	980	62.3
1B	-50	29800	54800	27.3	1107	63.7
3B	-50	29900	55600	29.8	1230	65.1
2B	-91	33500	56200	24.9	1002	63.1
4B	-90	33200	55300	25.1	1028	62.7
1C	78	33200	64800	18.8	913	57.3
6C	77	32100	65100	19.8	960	57.3
7C	33	33300	65500	19.9	1002	57.6
8C	33	34200	67300	20.2	1088	57.0
4C	-45	33400	72300	20.3	1113	53.0
5C	-40	32200	70700	21.2	1126	54.2
2C	-90	36200	73500	19.8	1043	50.8
3C	-90	34200	73300	22.8	1260	53.8

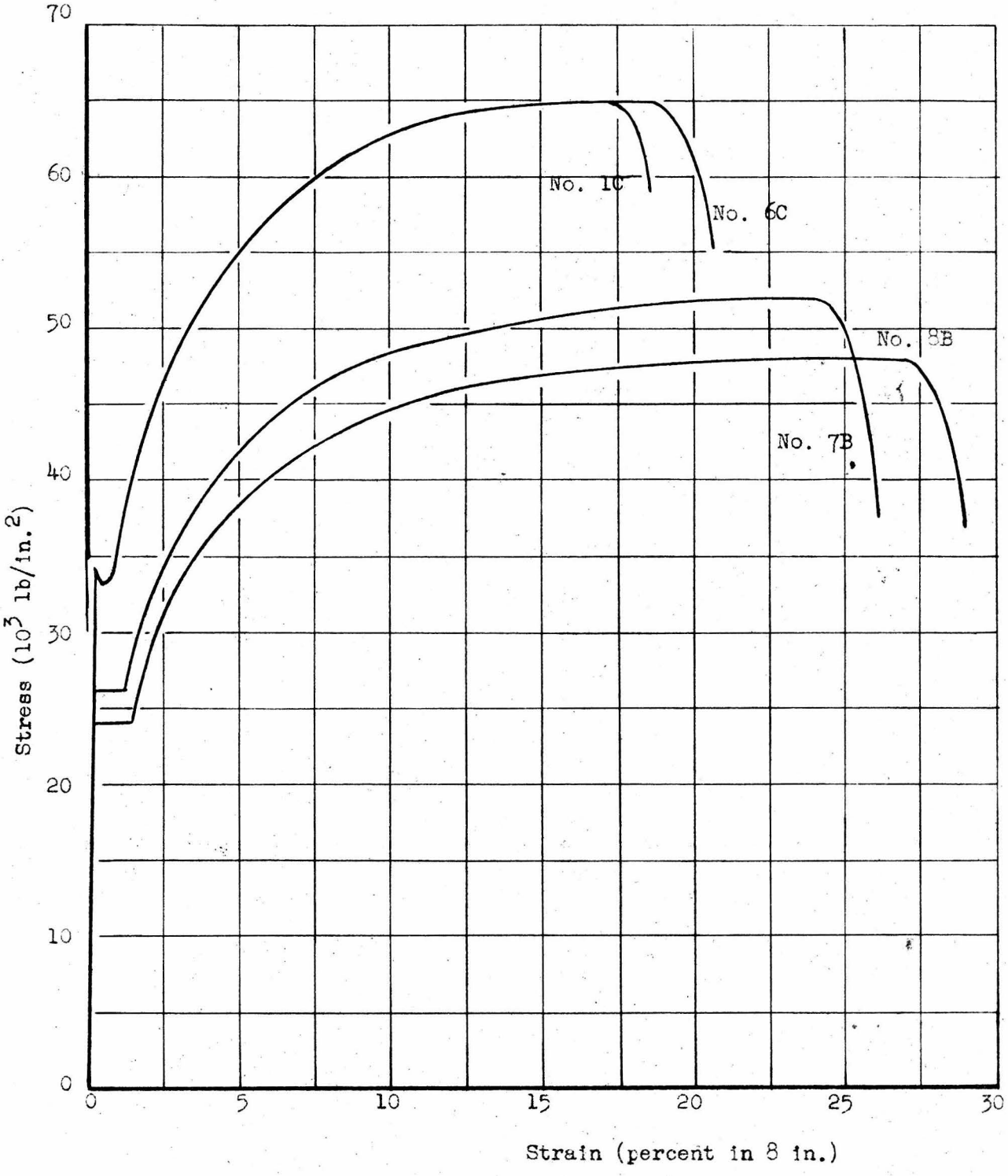

Fig. 14 Static stress-strain curves for ship plate steel at 77°F.

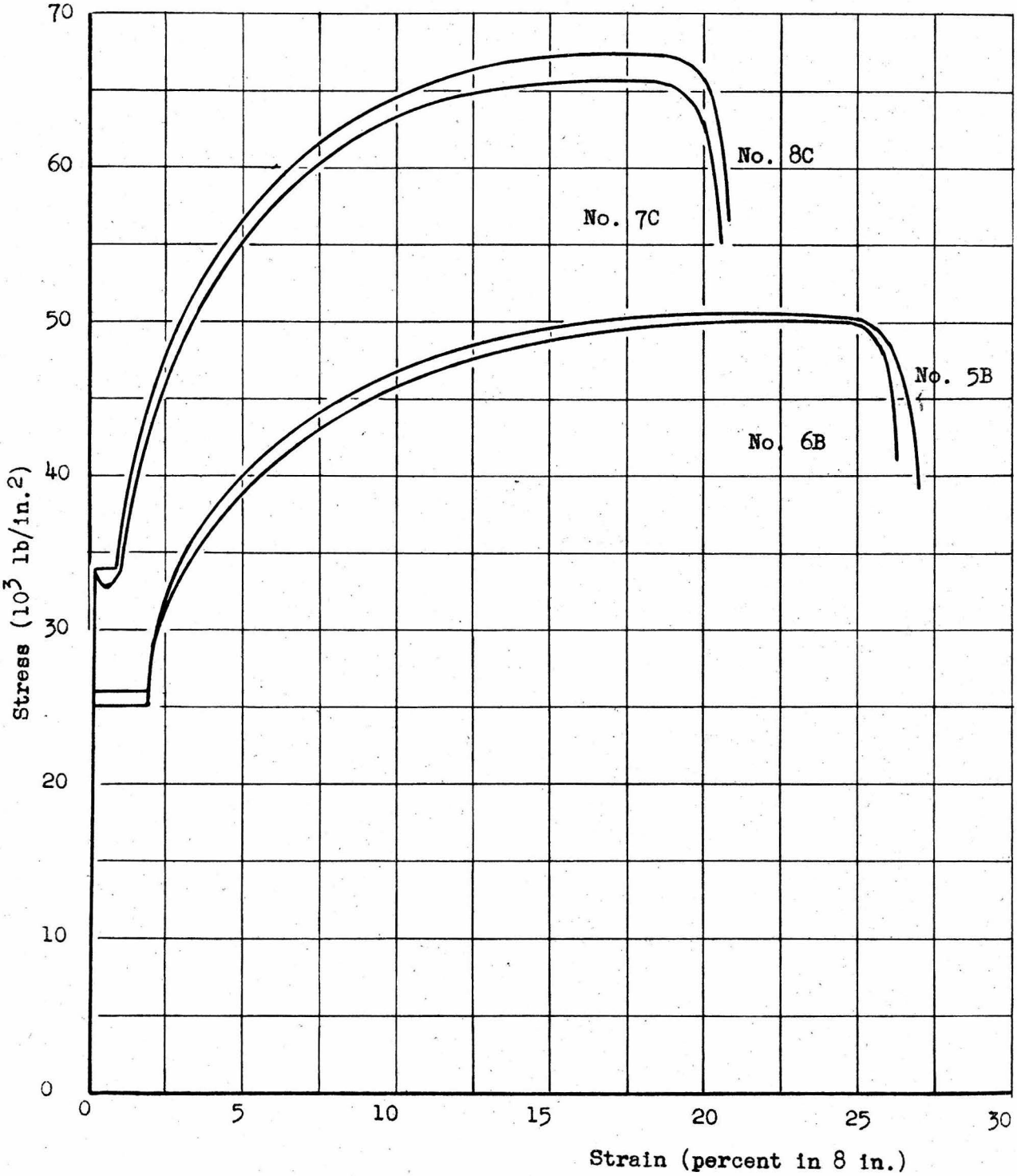

Fig. 15 Static stress-strain curves for ship plate steel at 32°F.

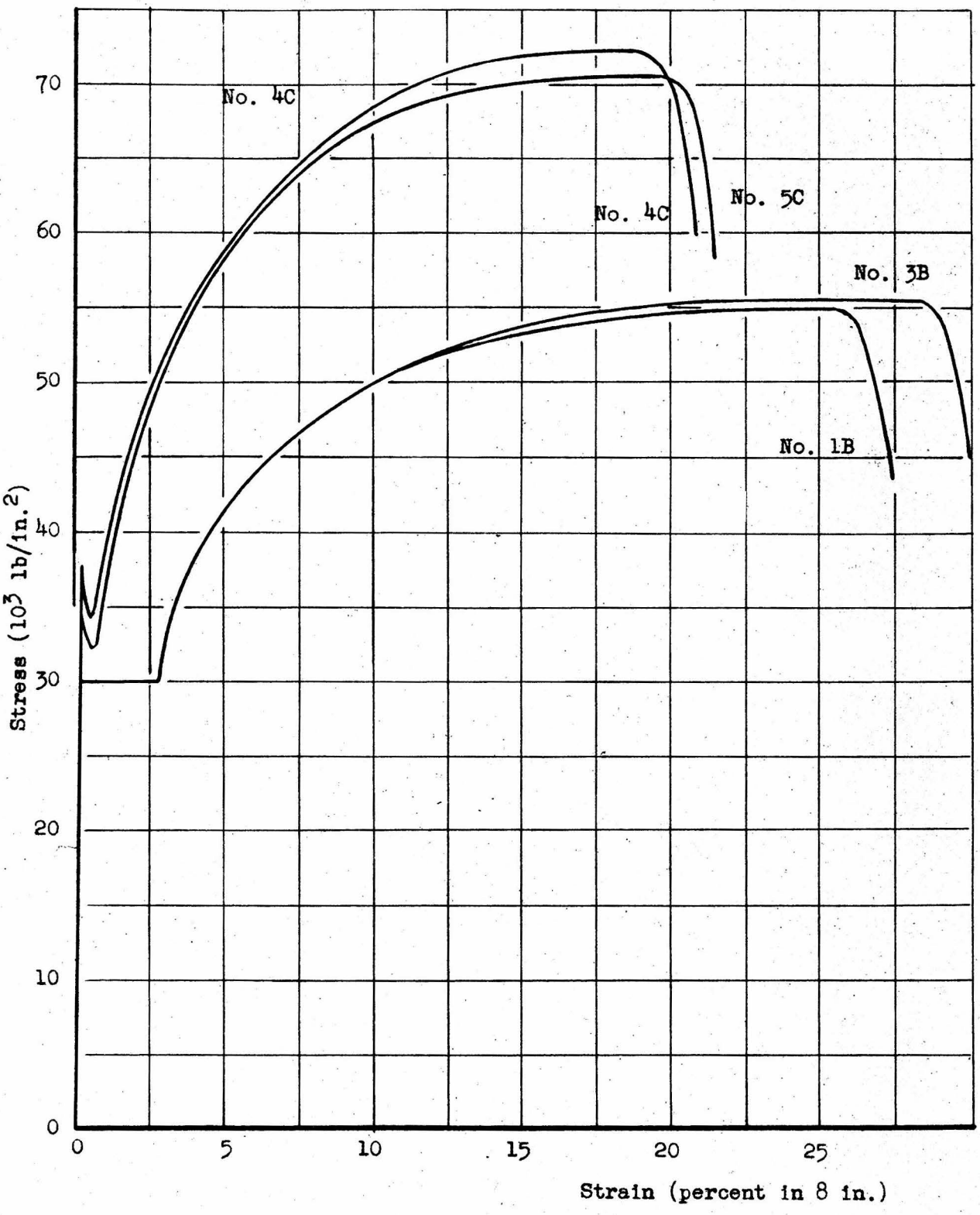

Fig. 16 Static stress-strain curves for ship plate steel at -45°F.

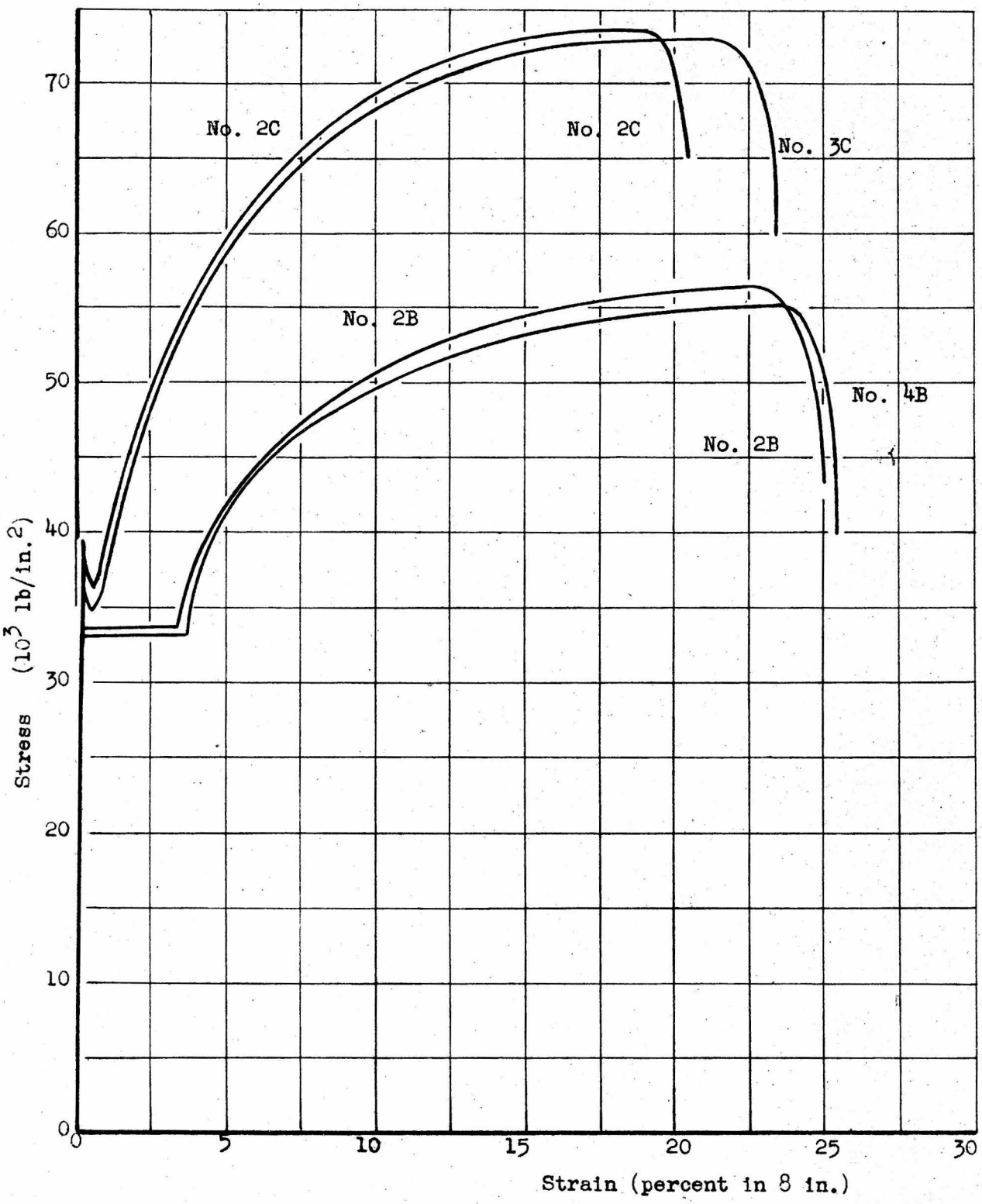

Fig. 17 Static stress-strain curves for ship plate steel at -90°F.

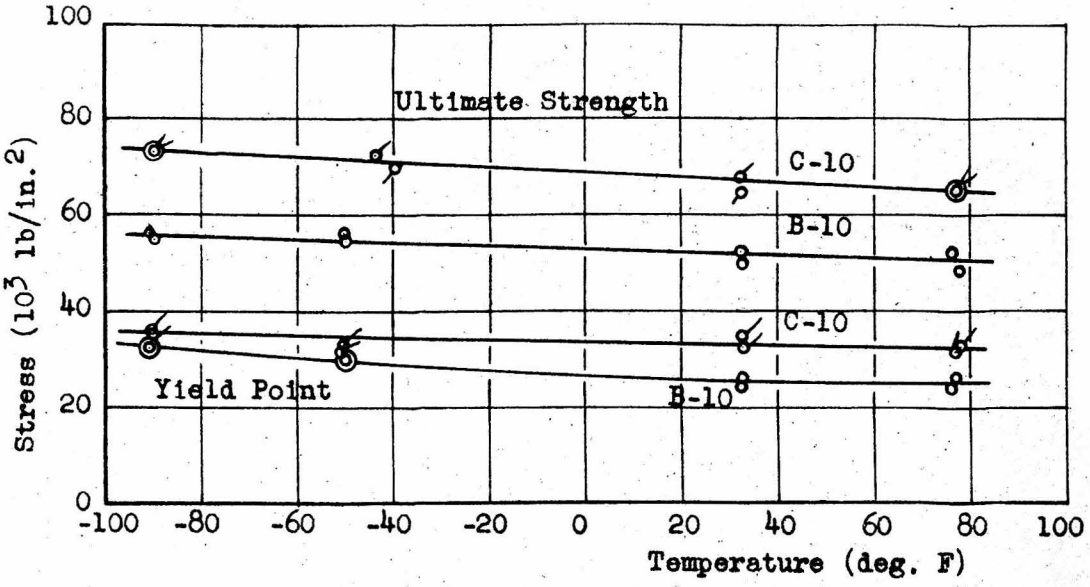

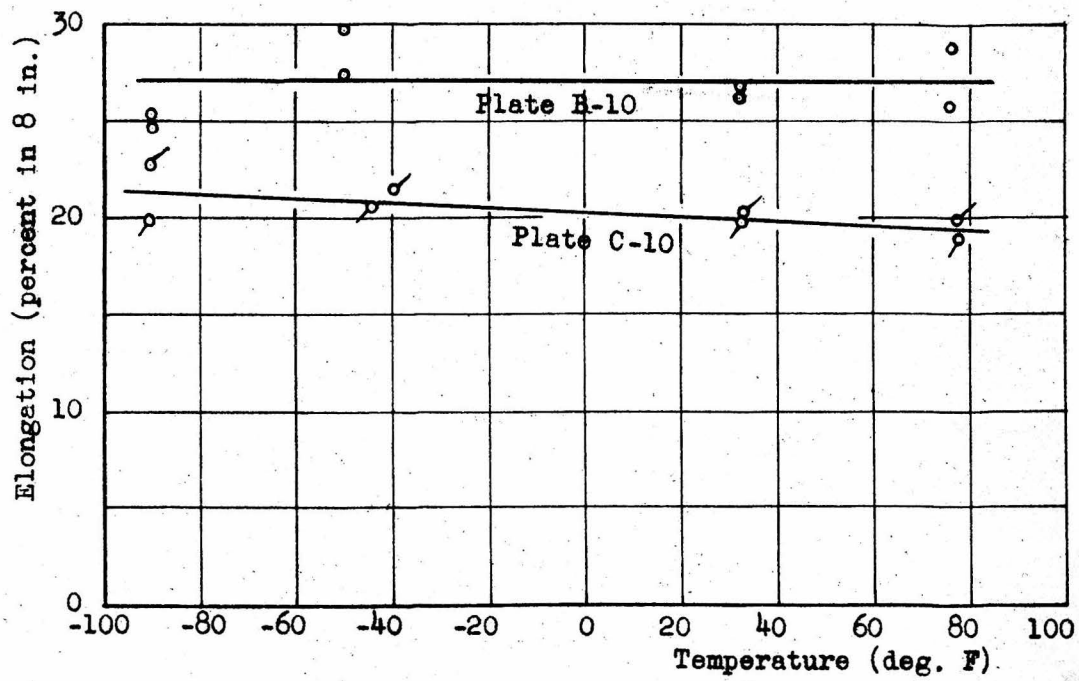

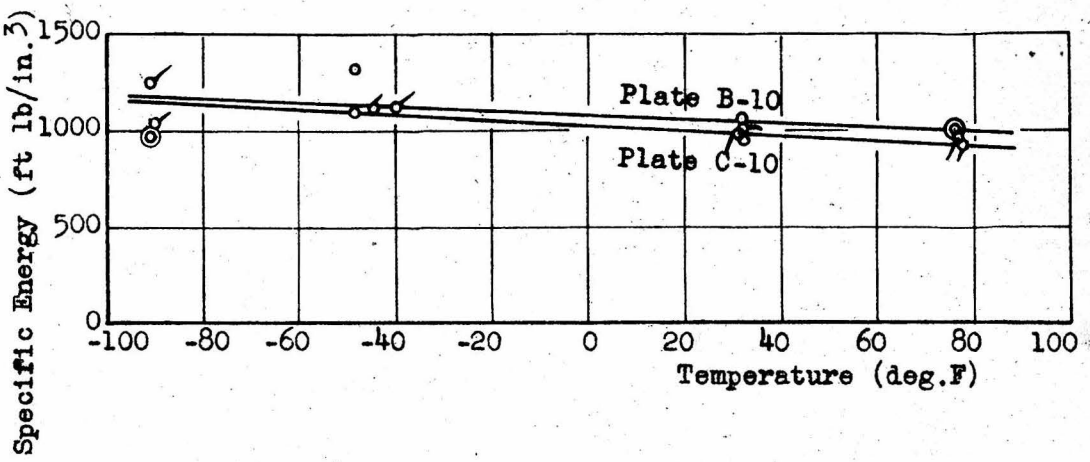

Fig. 18 Static ultimate strength, yield point, elongation, and specific energy each vs. temperature for ship plate steel.

TABLE II

RESULTS OF TENSION IMPACT TESTS ON SHIP PLATE STEEL B-10 at 75°F.

Spec. No.	Impact Velocity ft/sec	Ultimate Strength lb/in.^{2}	Elong. percent in 8 in.	Specific Energy ft lb/in.^{3}	Reduction of Area percent	Temp. deg. F
7B	Static	51800	25.8	1008	68.6	76
8B	Static	48200	28.7	1078	66.4	77
26B	24.8	56200	27.8	1260	66.6	71
37B	26.7	58900	28.7	1320	61.4	72
68B	40.8	63000	29.9	1490	68.0	73
24B	49.9	64100	25.6	1320	71.3	81
27B	50.7	63800	23.2	1180	63.8	71
36B	73.9	62600	23.8	1179	66.5	72
28B	74.2	*	23.8	*	66.1	71
20B	100.5	*	14.9	*	53.7	71
33B	101.0	*	20.1	*	64.0	76
35B	103.9	64100	16.4	832	65.4	72
34B	125.5	64000	12.9	640	66.3	72
21B	125.5	*	16.4	*	66.3	81
31B	147.2	65300	7.0	381	61.5	77
32B	149.8	*	11.1	*	69.2	72
22B	150.7	*	6.4	*	66.0	81
30B	170.0	57200	6.7	320	63.7	77
23B	172.3	*	7.3	*	64.9	81
40B	179.5	*	6.1	*	67.0	71.5
38B	179.8	54500	4.8	218	64.6	75
41B	197.0	54600	4.4	200	65.5	75
25B	202.1	53300	4.4	195	64.2	78
44B	202.2	58400	6.1	297	70.5	71.5
29B	206.9	58000	6.0	290	69.4	78

*No force-time record obtained for this test due to improper operation of the recording equipment.

TABLE III

RESULTS OF TENSION IMPACT TESTS ON SHIP PLATE STEEL B-10 at 35°F.

Spec. No.	Impact Velocity ft/sec	Ultimate Strength $lb/in.^2$	Elong. Percent in 8 in.	Specific Energy $ft\ lb/in.^3$	Reduction of Area percent	Temp. deg. F
5B	Static	51000	26.7	1020	66.4	31.5
6B	Static	50000	26.1	980	62.3	32.0
59B	24.3	65800	26.6	1360	70.0	35
56B	25.3	66400	29.5	1520	66.1	35
77B	41.0	*	25.3	*	61.5	33
60B	49.4	*	28.8	*	61.4	34
58B	49.4	68100	25.0	1350	63.1	34
61B	75.4	68700	18.6	1000	63.8	33
62B	77.4	68000	23.6	1270	63.2	33
63B	100.1	72000	20.2	1160	69.2	33
69B	101.0	71500	18.2	1020	60.9	33
72B	125.2	62200	8.0	420	60.3	33
71B	126.2	68600	9.0	510	60.3	33
74B	152.0	70400	6.4	360	60.2	34
73B	157.5	*	9.4	*	62.0	35
75B	180.3	75300	5.2	310	61.0	37
78B	200.1	64000	3.9	190	63.2	36
76B	200.6	*	3.3	*	60.7	34

*No force-time record obtained for this test due to improper operation of the recording equipment.

TABLE IV

RESULTS OF TENSION IMPACT TESTS ON SHIP PLATE STEEL B-10 AT ABOUT 0°F.

Spec. No.	Impact Velocity ft/sec	Ultimate Strength $lb/in.^2$	Elong. percent in 8 in.	Specific Energy $ft\ lb/in.^3$	Reduction of Area percent	Temp. deg. F.
90B	24.9	59800	28.2	1380	62.2	8
66B	25.1	66200	23.6	1280	61.6	-15
91B	25.6	63000	23.8	1210	70.7	6
57B	25.8	*	29.0	*	62.3	-22
102B	48.2	*	16.2	*	67.9	-28
67B	49.2	66500	20.0	1080	67.4	-12
92B	51.2	68200	20.2	1100	62.4	8
93B	52.2	67200	23.0	1250	67.0	9
94B	74.5	*	17.2	*	66.2	10
95B	75.3	*	18.8	*	59.8	10
98B	76.9	*	10.8	*	58.4	-15
101B	99.0	*	5.0	*	60.8	-17
99B	101.5	*	7.6	*	61.7	-8
96B	102.2	*	17.9	*	66.8	9
97B	104.0	*	16.1	*	63.4	13
100B	123.0	*	4.5	*	53.0	-21
19B	124.8	55100	4.9	258	56.2	-5

* No force-time record obtained for this test due to improper operation of the recording equipment.

TABLE V

RESULTS OF TENSION IMPACT TESTS ON SHIP PLATE STEEL B-10 at -40°F.

Spec. No.	Impact Velocity ft/sec	Ultimate Strength lb/in.^{2}	Elong. Percent in 8 in.	Specific Energy ft lb/in.^{3}	Reduction of Area percent	Temp. deg. F.
1B	Static	54800	27.3	1110	67.3	-50
3B	Static	55600	29.8	1230	65.1	-50
18B	9.1	*	11.8	*	63.4	-38
17B	20.2	69200	12.6	710	65.9	-38
9B	24.4	68700	12.1	650	65.7	-55
16B	37.0	68500	12.5	710	59.8	-44
10B	49.7	*	12.6	*	67.6	-50
15B	50.2	71100	11.6	700	67.8	-40
84B	61.0	69200	12.6	730	67.2	-45
88B	66.9	76000	14.5	900	66.9	-51
89B	73.2	72300	12.5	750	56.6	-41
11B	74.0	*	7.1	*	64.4	-43
14B	76.6	70400	6.0	352	61.4	-40
86B	99.4	82100	4.5	300	57.1	-50
12B	102.7	*	6.6	*	63.9	-44
47B	103.3	78200	4.7	290	58.4	-45
13B	103.6	*	3.2	*	57.0	-42
87B	120.7	78000	6.7	400	64.1	-44

* No force-time record obtained for this test due to improper operation of the recording equipment.

TABLE VI

RESULTS OF TENSION IMPACT TESTS ON SHIP PLATE STEEL B-10 at -70°F.

Spec. No.	Impact Velocity ft/sec	Ultimate Strength lb/in.^{2}	Elong. percent in 8 in.	Specific Energy ft lb/in.^{3}	Reduction of Area percent	Temp. deg. F.
2B	Static	56200	24.9	1022	63.1	-91
4B	Static	55300	25.1	1028	62.7	-90
55B	10.1	66000	14.4	790	61.4	-78
79B	11.1	66900	11.3	630	58.6	-77
54B	15.0	*	17.1	*	66.5	-82
43B	24.8	70700	8.7	520	62.1	-57
46B	26.3	73400	4.1	250	57.3	-70
80B	26.8	68400	10.5	600	57.8	-78
53B	30.8	71200	14.1	840	58.5	-72
42B	49.2	*	17.3	*	65.2	-63
45B	50.2	71600	9.3	550	62.8	-71
81B	50.2	72000	11.3	700	60.5	-76
49B	50.4	71200	9.1	550	64.4	-66
51B	73.4	80600	10.2	680	67.3	-76
48B	76.9	75800	9.7	610	58.3	-68
83B	89.2	84800	4.5	320	59.5	-72
50B	99.4	82000	4.5	300	59.0	-70
82B	122.3	*	3.6	*	56.2	-70
52B	130.5	83200	4.1	235	62.2	-70

* No force-time record obtained for this test due to improper operation of the recording equipment.

TABLE VII

RESULTS OF TENSION IMPACT TESTS ON SHIP PLATE STEEL C-10 at 75°F.

Spec. No.	Impact Velocity ft/sec	Ultimate Strength lb/in.^{3}	Elong. percent in 8 in.	Specific Energy ft lb/in.^{3}	Reduction of Area Percent	Temp. deg. F.
1C	Static	64800	18.8	913	57.3	78
6C	Static	65100	19.8	960	57.3	77
53C	25.4	76300	25.8	1591	58.8	74
39C	26.4	70200	25.4	1360	59.3	73
52C	50.2	70100	28.8	1630	62.4	74
43C	50.3	78800	26.3	1679	67.5	73
40C	50.4	78500	34.2	2130	61.6	73
63C	51.2	*	20.8	*	58.4	68
51C	72.5	76200	26.9	1660	60.9	74
81C	73.8	80000	23.7	1520	56.6	73
41C	75.4	82600	22.3	1464	57.5	73
90C	87.7	*	16.0	*	53.7	70
50C	101.0	78700	27.0	1718	60.3	74
42C	102.2	78400	22.8	1407	61.4	73
35C	125.0	*	20.0	*	55.9	70
36C	127.5	*	17.8	*	55.7	80
44C	147.8	82200	17.0	1090	57.6	73
49C	154.2	86000	17.7	1190	60.3	74
46C	173.8	82700	13.9	901	59.7	74
45C	176.8	81700	15.4	977	58.4	74
48C	199.9	76000	11.5	699	57.7	74
47C	202.6	64700	8.0	391	68.2	74

*No force-time record obtained for this test due to improper operation of the recording equipment.

TABLE VIII

RESULTS OF TENSION IMPACT TESTS ON SHIP PLATE STEEL C-10 AT 35°F.

Spec. No.	Impact Velocity ft/sec	Ultimate Strength $lb/in.^2$	Elong. percent in 8 in.	Specific Energy $ft\ lb/in.^3$	Reduction of Area percent	Temp. °F
7C	Static	65500	19.9	1002	57.6	33
8C	Static	67300	20.2	1088	57.0	33
62C	24.6	*	27.1	*	60.4	33
72C	24.9	74700	19.9	1180	61.2	34
26C	25.1	*	23.0	*	58.1	33
10C	25.3	*	21.7	*	60.5	33
9C	25.8	*	20.0	*	57.6	34
74C	49.5	80300	23.9	1540	56.7	37
11C	50.3	*	24.2	*	61.6	34
25C	50.3	*	22.1	*	59.4	35
64C	52.2	*	27.8	*	61.0	33
24C	74.4	*	22.5	*	60.7	34
75C	74.8	78000	25.2	1600	60.0	37
12C	75.9	*	24.1	*	61.6	34
65C	76.2	*	24.5	*	60.6	33
76C	98.9	81700	19.7	1270	60.3	36
16C	99.1	*	18.9	*	60.5	34
23C	99.7	*	17.1	*	59.4	33
66C	101.6	*	23.9	*	59.3	33
22C	124.1	*	20.8	*	56.8	33
17C	125.6	*	15.4	*	58.3	34
67C	127.5	*	18.8	*	58.4	33
77C	129.4	83000	22.5	1510	59.2	40
68C	145.3	*	17.1	*	65.0	37
15C	150.8	*	13.9	*	60.8	34
21C	150.9	*	14.4	*	57.2	35
78C	154.6	86500	22.8	1580	57.0	46
20C	174.1	*	8.5	*	59.0	37
69C	176.0	*	11.7	*	56.2	35
84C	177.0	76700	10.7	680	58.9	34
19C	178.8	*	9.4	*	56.5	36
71C	194.7	*	8.7	*	56.4	37
13C	199.5	*	6.9	*	57.2	35
85C	201.8	85200	7.5	500	57.5	35
14C	202.2	*	6.3	*	58.9	36

*No force-time record obtained for this test due to improper operation of the recording equipment.

TABLE IX

RESULTS OF TENSION IMPACT TESTS ON SHIP PLATE STEEL C-10 AT -40°F.

Spec. No.	Impact Velocity ft/sec	Ultimate Strength $lb/in.^2$	Elong. percent in 8 in.	Specific Energy $ft\ lb/in.^3$	Reduction of Area percent	Temp. deg. F
4C	Static	72300	20.3	1113	53.0	-45
5C	Static	70700	21.2	1126	54.2	-40
70C	10.6	72400	19.5	1100	58.8	-41
80C	24.4	79500	20.3	1320	60.1	-45
33C	25.2	*	13.0	*	57.2	-51
34C	49.1	*	12.9	*	56.1	-35
31C	49.6	78500	12.7	795	52.3	-32
73C	51.0	87800	20.7	1480	57.9	-42
30C	75.4	*	9.2	*	56.8	-35
93C	75.5	84500	22.1	1530	56.6	-42
79C	99 0	88000	14.4	1050	59.0	-49
27C	105.1	79000	9.6	632	58.0	-30
32C	117.8	*	8.0	*	55.6	-16 #
96C	125.6	88500	14.2	1050	55.4	-42
29C	127.6	*	6.6	*	57.7	+2 #
89C	147.6	89500	8.5	590	56.6	-43
94C	151.0	84500	8.8	620	53.0	+5 #
82C	174.1	85700	7.0	480	56.4	-37

* No force-time record obtained for this test due to improper operation of the recording equipment.

System warmed up just before the test.

TABLE X

RESULTS OF TENSION IMPACT TESTS ON SHIP PLATE STEEL C-10 AT -70°F.

Spec. No.	Impact Velocity ft/sec	Ultimate Strength lb/in.^{2}	Elong. percent in 8 in.	Specific Energy ft lb/in.^{3}	Reduction of Area percent	Temp. deg. F.
2C	Static	73500	19.8	1043	50.8	-90
3C	Static	73300	22.8	1260	53.8	-90
54C	10.4	*	16.5	*	58.0	-74
55C	15.9	*	15.2	*	53.5	-75
56C	26.6	86700	16.0	1090	54.8	-72
57C	26.9	86200	17.4	1240	56.0	-73
58C	49.8	84500	13.1	920	55.6	-55
59C	49.8	88800	15.8	1110	60.0	-70
60C	74.7	92000	16.6	1270	55.2	-72
61C	76.7	93100	17.4	1340	54.4	-66
88C	85.1	89300	18.5	1350	58.2	-61
92C	95.2	92200	13.5	1050	55.6	-74
87C	102.0	#	0	#	0	-68
86C	102.3	#	0	#	0	-67
91C	111.7	88200	12.0	880	55.7	-68
83C	120.0	#	0	#	0	-58
99C	122.2	90500	8.5	630	55.8	-71
100C	126.5	#	0	#	0	-65
101C	137.8	#	0.5	#	6.3	-68

* No force-time record obtained for this test due to improper operation of the recording equipment.

No force-time record obtained due to brittle type fracture at the moving-end of the specimen.

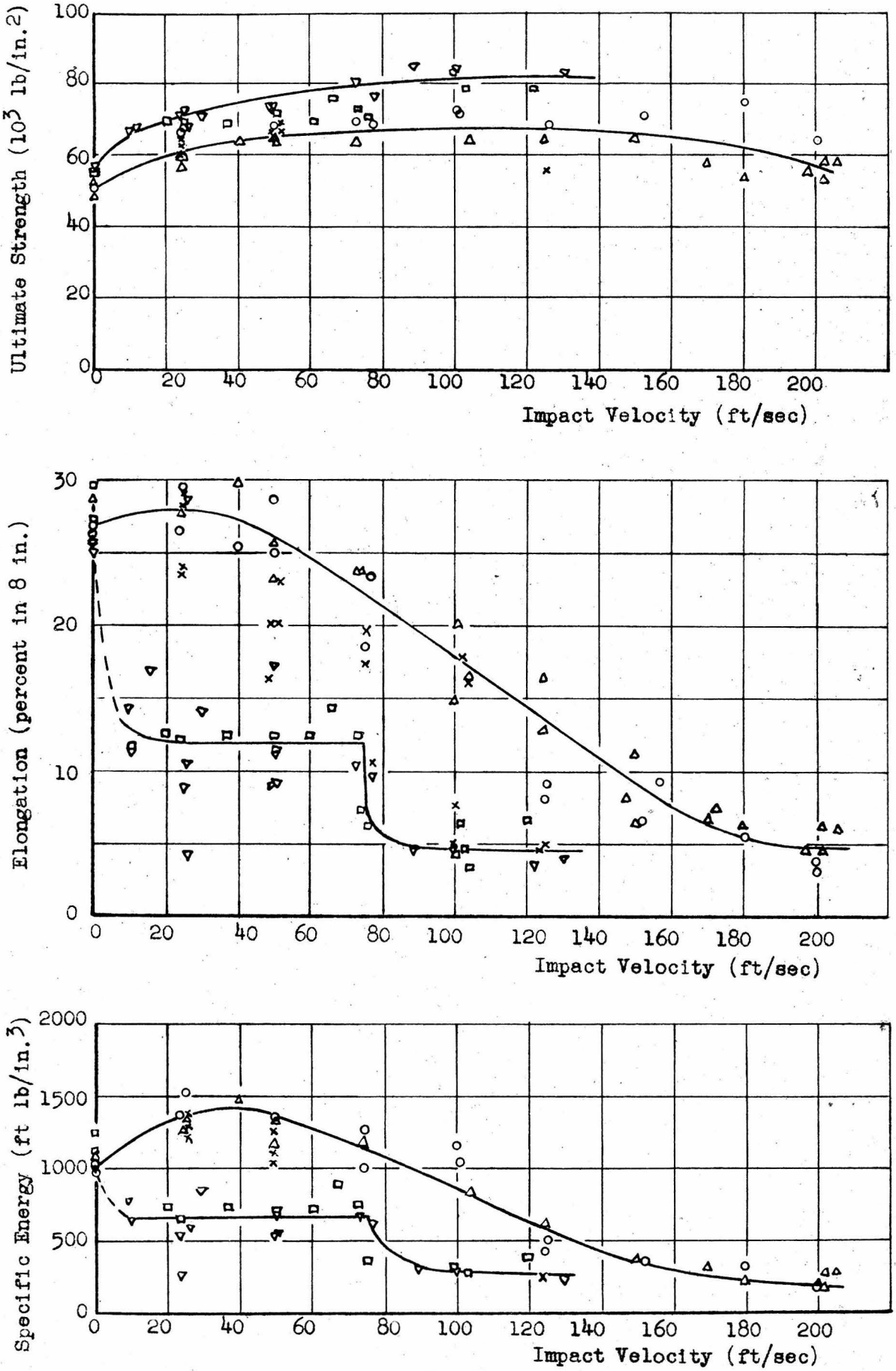

Fig. 19 Ultimate strength, elongation, and specific energy each vs. impact velocity at 75°F (△), 35°F (○), 0°F (x), -40°F (□), and -70°F (▽) for ship plate steel B-10.

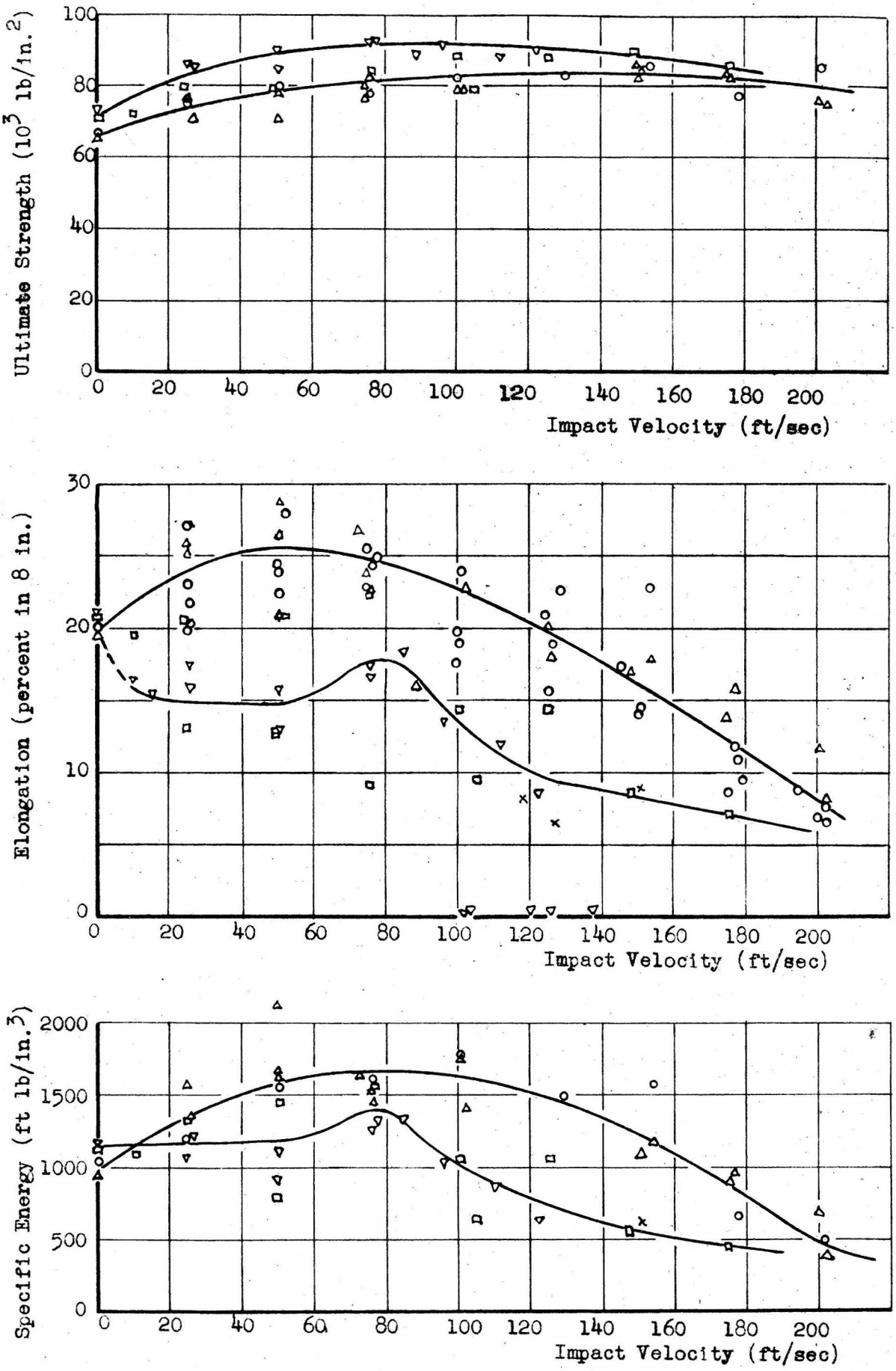

Fig. 20 Ultimate strength, elongation, and specific energy each vs. impact velocity at 75°F (△), 35°F (○), 0°F (x), -40°F (□), and -70°F (▽) for ship plate steel C-10.

similarity of the data, a single curve was passed through the points for the 75°F and 35°F and another curve through the -40°F and -70°F points. Tests were made on a few plate B-10 specimens at about 0°F to determine the nature of the transition between the two temperature ranges.

The reduction of area is 5 to 10 percent lower at the low temperatures, but is not affected by impact velocity.

The ultimate strength increases with increasing impact velocity to approximately a constant value above 75 ft/sec. This constant value is about 40 percent above static values for plate B-10 and 20 percent above static values for plate C-10. The impact ultimate strength of plate B-10 is increased about 20 percent, and of plate C-10 about 12 percent as the temperature is lowered from room temperature to -70°F.

The variation of elongation with impact velocity, within the temperature range covered by this investigation, is similar for the two ship plate steels studied. The curves for tests made at the room temperatures show an increase of elongation with increasing impact velocity followed by a gradual decrease. The curves for tests made at -40°F and -70°F show an immediate drop in elongation from static tests to tests at low impact velocities, and then show nearly constant values of elongation until a certain critical velocity is reached, followed by a rapid decrease to a minimum value. This result is similar to that obtained on preliminary tests [18] with annealed 0.19 percent carbon steel.

Five of the seven tests made with specimens from plate C-10 at -70°F at impact velocities higher than 100 ft/sec exhibited a brittle fracture at the tup-end fillet with no measurable elongation.

Fig. 21 presents a comparison between the structure at the fracture of specimens exhibiting brittle and ductile failure under similar conditions of loading. In Fig. 21 (a) the failure appears to have occured by cleavage and passes through the grains with little or no deformation. The dark streak is a crack extending into the specimen from the face of the fracture. Fig. 21 (b) shows a structure characteristic of a normal ductile fracture with severe elongation of the grains near the fracture surface.

Curves of specific energy vs. impact velocity reflect the trend of elongation because the ultimate strength is essentially constant.

The variation of elongation with temperature for each of the impact velocities used is shown in Figs. 22 and 23. These curves show that for any specified impact velocity, the principal decrease in elongation with decreasing temperature occurs within a fairly narrow transition range.

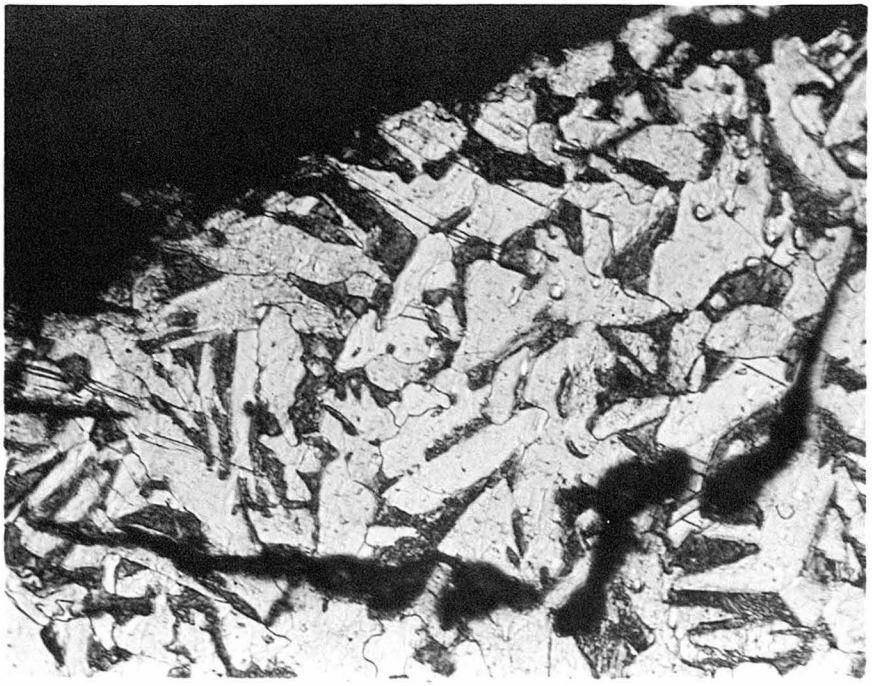

(a) Specimen 87c, brittle fracture at -68°F at impact velocity of 102.0 ft/sec. Nital etch, X300.

(b) Specimen 92c, ductile fracture at -74°F at impact velocity of 95.2 ft/sec. Nital etch, X300.

Fig. 21 Photomicrographs of tensile impact fractures of ship plate steel C-10 at low temperatures.

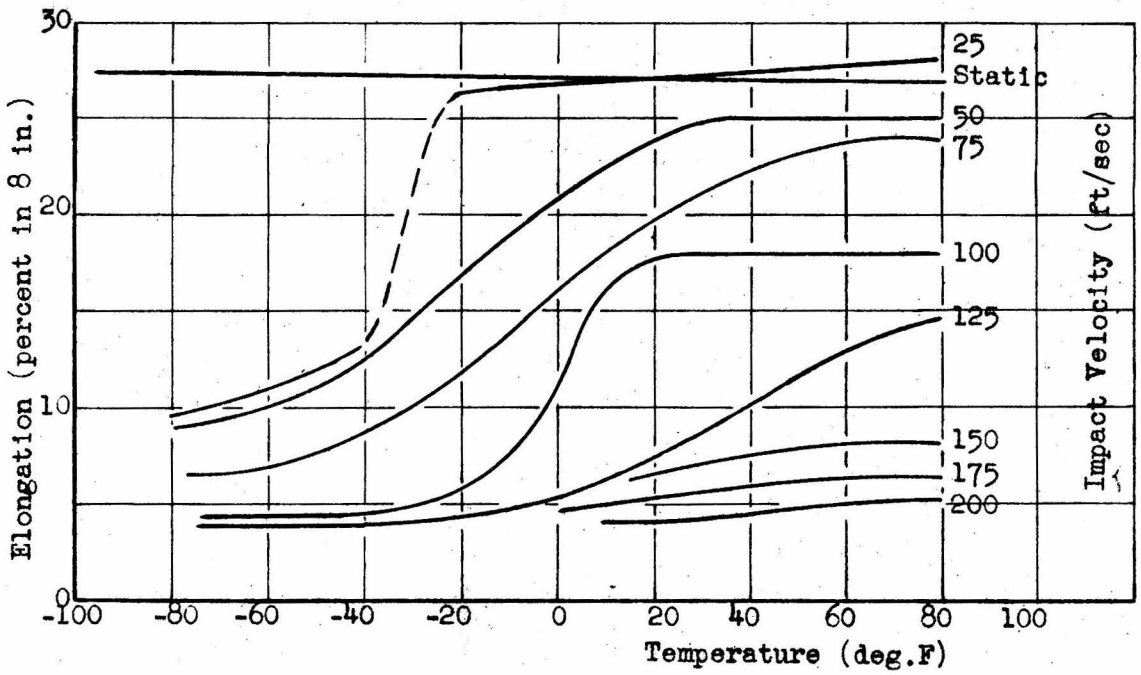

Fig. 22 Curves of elongation vs. temperature for B-10 ship plate steel at different impact velocities.

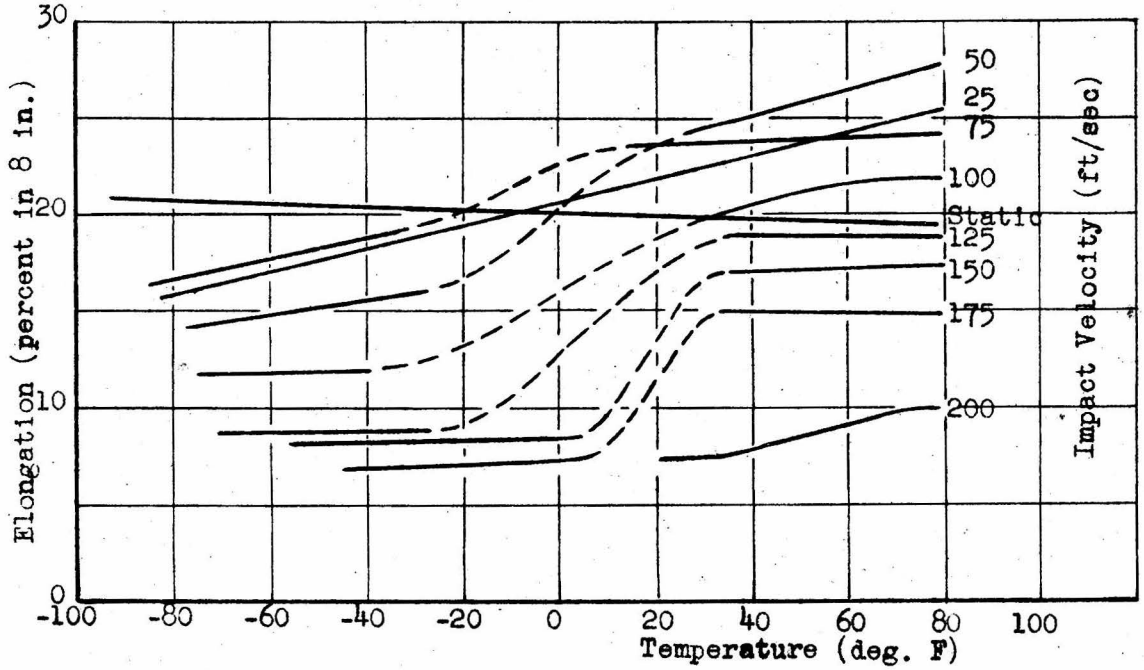

Fig. 23 Curves of elongation vs. temperature for C-10 ship plate steel at different impact velocities.

DISCUSSION OF RESULTS

The slight decrease of ultimate strength obtained from some tests at impact velocities above 150 ft/sec is probably due to the character of the force-time record rather than to a change in properties.

In the force-time records of all tests of impact velocities of 150 ft/sec or higher, where there has been sufficient elongation that the record includes four or more cycles of dynamometer vibration, the average value of the first 2, 3, or 4 cycles on the record is lower than the average of the subsequent oscillations. The average height of the record after the first four cycles has been taken as the force corresponding to the ultimate strength wherever possible. This effect can be seen in Fig. 13 (b), (c).

A scattering from the smooth curve of points obtained for ultimate strength is expected from the estimated ± 10 to ± 20 percent possible measuring error. However, only 12 points differed from the curves by more than 10 percent and all but one of these 12 were from tests at high velocities with small elongation.

The decrease of percentage elongation with increasing impact velocity can be explained by the decrease of velocity of plastic strain propagation. The decrease of elongation with decreasing temperature for any impact velocity shown in Figs. 22 and 23 cannot be explained so easily. One explanation

may be that the shape of the dynamic stress-strain relation may be affected by temperature and that a transition from the room temperature relation to the low temperature relation occurs between 35°F and -40°F, and that the relation is such that the velocity of plastic strain propagation is reduced at low temperatures.

The scattering in values of percentage elongation is very wide. This effect is inherent in any tension test and is caused by natural variation from one specimen to another. In addition to this, in tensile impact tests the final strain distribution may vary widely from one specimen to another, because of the inconsistency of strain wave reflections from the ends of the specimen.

In the range of impact velocities and temperatures covered in this investigation, the elongation in the necked down portion of the specimens is nearly constant. This elongation amounts to about 5 percent in 8 in., and is the reason that the minimum value of percentage elongation obtained in all tests except the five with brittle fractures is about 5 percent.

The occurence of the brittle fracture, obtained in some of the low temperature, high velocity tests on C-10, might be explained by the relation between critical slip and cleavage stress caused by the constraint of the tup-end

shoulder and by the elastic strain wave corresponding to the impact velocity which would have returned to the moving-end shoulder 0.08×10^{-3} sec after the impact. This explanation is weakened by the fact that some of the impact tests exhibited ductile fractures and that the specimens were extremely ductile under static conditions. This would indicate that the low temperature behavior of this material is influenced by impact velocity, strain rate, and perhaps other factors. No satisfactory explanation has been found.

Curves of specific energy vs. impact velocity are used to determine the engineering critical impact velocity. From an examination of Fig. 19, the engineering critical impact velocity of ship plate B-10 is found to be about 50 ft/sec at room temperature and about 75 ft/sec at low temperatures, and from Fig. 20 that of plate C-10 is found to be about 90 ft/sec at room temperature and at low temperatures. While the engineering velocity of these samples of ship plate may be about the same or slightly higher at low temperatures, the energy to produce rupture is much lower at the low temperatures. The velocity for zero strain propagation is determined from the elongation vs. impact velocity curves, as the point that first reaches the minimum elongation. This is at about 190 ft/sec at room temperature and about 90 ft/sec at low temperatures for plate B-10, and above 200 ft/sec at room temperature and about 140 ft/sec at low temperatures for plate C-10. These different critical velocities are shown plotted against temperature in Fig. 24.

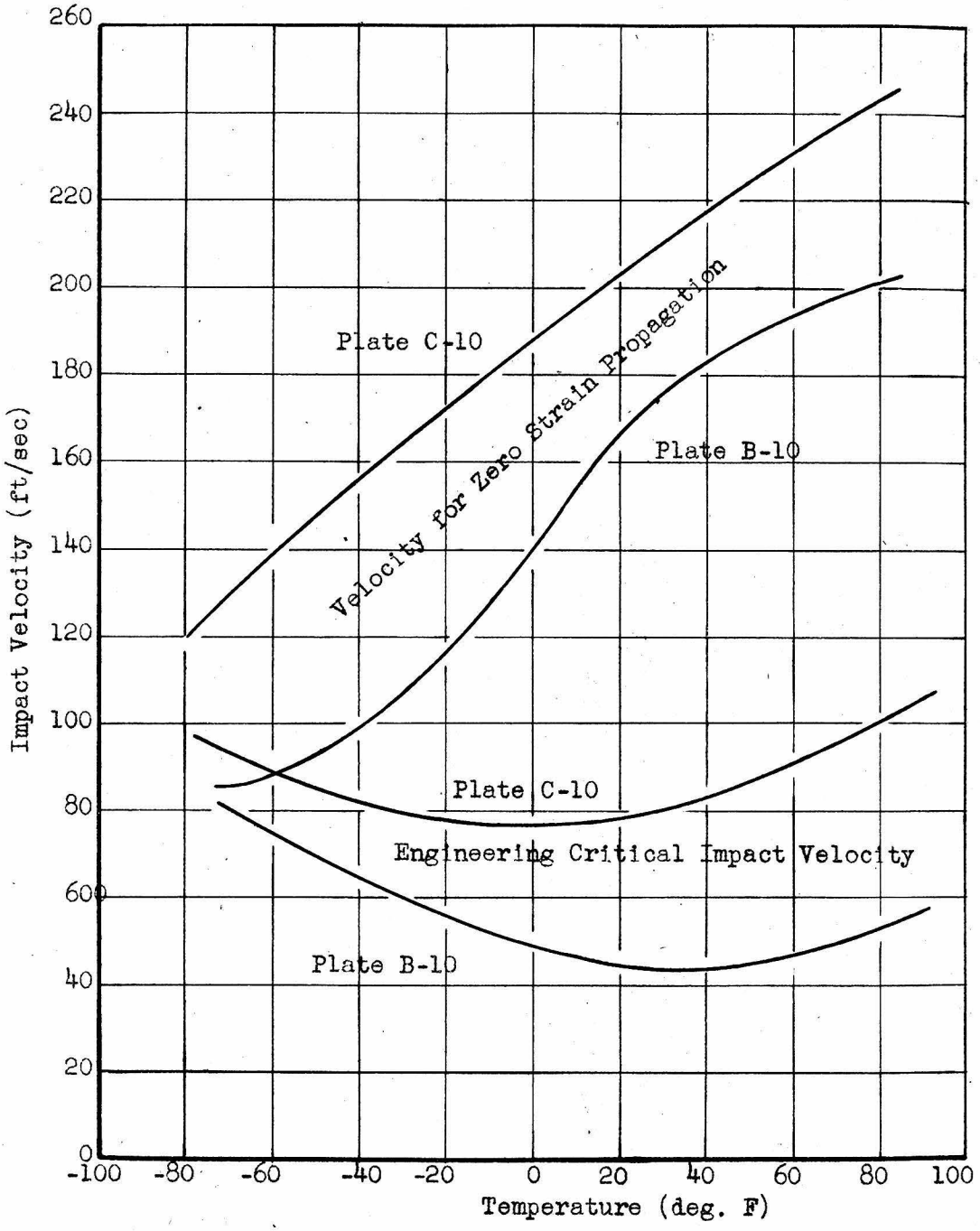

Fig. 24 Engineering critical impact velocity and velocity for zero strain propagation vs. temperature for ship plate steel.

SUMMARY

The results of this investigation on two types of medium steel ship plate can be summarized as follows:

1. The static yield point, ultimate strength, and specific energy increase with decreasing temperature.
2. The static elongation remains essentially constant with decreasing temperature.
3. The static reduction of area decreases slightly with decreasing temperature.
4. In tensile impact tests, ultimate strength increases with increasing impact velocity and decreasing temperature.
5. Elongation and specific energy remain constant or increase with increasing impact velocity depending on temperature, and above a certain critical velocity, decrease with increasing impact velocity. Elongation and specific energy decrease with decreasing temperature for any impact velocity, the greatest decrease is between 35°F and -40°F.
6. Reduction of area is not affected by impact velocity, but is slightly reduced by decreasing temperature.
7. The engineering critical impact velocity increases slightly with decreasing temperature for plate B-10 and remains about constant for plate C-10. The velocity

for zero strain propagation decreases with decreasing temperature for both ship plate steels.

8. The reasons are not known for the decrease in tensile impact elongation with decreasing temperature for both materials, and the brittle failure of some specimens of plate C-10 at low temperature and high impact velocity, but may be due to the effect of temperature on the relative stresses for slip and cleavage in mild steel, and may be associated with the relations of impact velocity, strain rate, and temperature.

9. On the basis of this investigation it can be concluded that plate C-10 would be more satisfactory than plate B-10 for use under conditions of longitudinal impact at low temperature because of higher energy absorption and higher critical impact velocity. However, when using plate C-10, caution should be exercised and conditions of high velocity impact be avoided at temperatures below -40°F, because of the possibility of brittle fracture with very low energy absorption. Plate B-10 does not exhibit this brittle fracture characteristic.

REFERENCES

1. "Metals Handbook," American Society for Metals, Cleveland, (1939), p. 86-97. (With 46 references).

2. H.W. Gillett, "Impact Resistance and Tensile Properties of Metals at Subatmospheric Temperatures," Am. Soc. Testing Mats., Philadelphia, (August 1941). (With 83 references).

3. H.W. Gillett and F.T. McGuire, "Behavior of Ferritic Steels at Low Temperatures: Parts I and II," Am. Soc. Testing Mats., (December 1945).

4. C.S. Barrett, "Structure of Metals," McGraw-Hill Book Co., New York, (1943), p. 322.

5. H.C. Mann, "High Velocity Tension Impact Tests," Proceedings, Am. Soc. Testing Mats., (1936), Vol. 36, Part II, p. 85.

6. H.C. Mann, "Fundamental Study of the Design of Impact Test Specimens," Proceedings, Am. Soc. Testing Mats., (1937), Vol. 37, Part II, p. 102.

7. D.S. Clark and G. Datwyler, "Stress-Strain Relations Under Tension Impact Loading," Proceedings, Am. Soc. Testing Mats., (1938), Vol. 38, p. 98.

8. D.S. Clark, "The Influence of Impact Velocity on the Tensile Characteristics of Some Aircraft Metals and Alloys," Nat. Advisory Comm. Aero., Tech. Notes No. 868, (October 1942).

9. M. Manjoine and A. Nadai, "High Speed Tension Tests at Elevated Temperatures," Proceedings, Am. Soc. Testing Mats., (1940), Vol. 40, p. 822; Transactions, Am. Soc. Mechanical Engrs., Journal of Applied Mechanics, (1941), Vol. 8, No. 2, p. A-77.

10. A.V. De Forest, C.W. MacGregor, and A.R. Anderson, "Rapid Tension Tests Using the Two-Load Method," Metals Technology, (December, 1941), p. 1.

11. E.R. Parker and C. Ferguson, "The Effect of Strain Rate Upon the Tensile Impact Strength of Some Metals," Transactions, Am. Soc. Metals, (1942), Vol. XXX, p. 68.

12. Th. von Kármán, "On the Propagation of Plastic Deformation in Solids," Nat. Defense Res. Comm. Report No. A-29 (O.S.R.D. No. 365), (February 1942).

13. Th. von Kármán and Pol Duwez, "On the Propagation of Plastic Strains in Solids," Presented at Sixth Int. Congress for App. Mech., Paris, (September 1946).

14. D.S. Clark, "Final Summary Report on the Behavior of Metals Under Dynamic Conditions," Nat. Defense Res. Comm. Report No. M-492 (O.S.R.D. No. 4868), (March 1945). (With 33 reports as references).

15. P.E. Duwez and D.S. Clark, "An Experimental Study of the Propagation of Plastic Deformation Under Conditions of Longitudinal Impact," Am. Soc. Testing Mats., (1947), Vol. 47, p. 502.

16. P.E. Duwez, D.S. Wood, and D.S. Clark, "The Propagation of Plastic Strain in Tension," Nat. Defense Res. Comm. Report No. A-99 (O.S.R.D. No. 931), (September 1942).

17. H.F. Bohenblust, J.V. Charyk, and D.H. Hyers, "Graphical Solutions for Problems of Strain Propagation in Tension," Nat. Defense Res. Comm. Report No. A-131 (O.S.R.D. No. 1204), (February 1943).

18. D.A. Elmer and D.S. Clark, "A Preliminary Investigation of the Influence of Low Temperature on the Critical Impact Velocity of Steel," Submitted to the David Taylor Model Basin, Washington, D.C., (August 1947).

19. Thomas Young, "Course of Lectures on Natural Philosophy...," (1807), Vol. 1, p. 135.

20. P.E. Duwez, H.E. Martens, D.A. Elmer, and D.S. Clark, "The Influence of Pure Strain Rate on the Tensile Properties of Three Types of Ship Plate," Nat. Defense Res. Comm. No. M-495 (O.S.R.D.-4773), (February 1945).

21. P.E. Duwez, H.E. Martens, and D.S. Clark, "A Preliminary Study of the Influence of Rapid Loading and Time at Load on the Initiation of Plastic Deformation in Tension," Nat. Defense Res. Comm. Report No. M-450 (O.S.R.D. No. 4621), (February 1945).

22. P.E. Duwez, D.S. Wood, and D.S. Clark, "The Influence of Specimen Length on Strain Propagation in Tension," Nat. Defense Res. Comm. Report No. A-105 (O.S.R.D. No. 957), (November 1942).

23. P.E. Duwez, D.S. Wood, and D.S. Clark, "The Influence of Specimen Dimensions and Shape on the Results of Tensile Impact Tests," Nat. Defense Res. Comm. Report No. A-237 (O.S.R.D. No. 3028), (December 1943).

24. W.R. Campbell, "Performance Tests of Wire Strain Gages: Part VI, Effect of Temperature on Calibration Factor and Gage Resistance," Nat. Advisory Comm. Aero., Tech. Notes No. 1456, (January 1948).